The dark and visible matter content of low surface brightness disk galaxies

Blok, W. J. G. de; McGaugh, S. S.

Published in:
The Astrophysical Journal

Publication date:
1997

Citation for published version (APA):
Blok, W. J. G. D., & McGaugh, S. S. (1997). The dark and visible matter content of low surface brightness disk galaxies. The Astrophysical Journal, 477(2).

The dark and visible matter content of low surface brightness disk galaxies

W.J.G. de Blok[1] and S.S. McGaugh[2]

[1] *Kapteyn Astronomical Institute, P.O. Box 800, 9700 AV Groningen, The Netherlands*
[2] *Department of Terrestrial Magnetism, Carnegie Institution of Washington, 5241 Broad Branch Road NW, Washington, DC 20015, USA*

ABSTRACT

We present mass models of a sample of 19 low surface brightness (LSB) galaxies and compare the properties of their constituent mass components with those of a sample of high surface brightness (HSB) galaxies. We find that LSB galaxies are dark matter dominated. Their halo parameters are only slightly affected by assumptions on stellar mass-to-light ratios. Comparing LSB and HSB galaxies we find that mass models derived using the maximum disk hypothesis result in the disks of LSB galaxies having systematically higher stellar mass-to-light ratios than HSB galaxies of similar rotation velocity. This is inconsistent with all other available evidence on the evolution of LSB galaxies. We argue therefore that the maximum disk hypothesis does not provide a representative description of the LSB galaxies and their evolution. Mass models with stellar mass-to-light ratios determined by the colors and stellar velocity dispersions of galactic disks imply that LSB galaxies have dark matter halos that are more extended and less dense than those of HSB galaxies. Surface brightness is thus related to the halo properties. LSB galaxies are slowly evolving, low density and dark matter dominated galaxies.

Key words: dark matter — galaxies: kinematics and dynamics — galaxies: spiral — galaxies: fundamental parameters — galaxies: halos

1 INTRODUCTION

The discrepancy between the amount of matter implied by the Hɪ rotation curves of spiral galaxies and the amount of matter actually observed (in the form of stars and gas) is usually interpreted as dark matter (DM) halos that surround the directly observable parts of galaxies, although alternative theories of modified Newtonian dynamics (Milgrom 1983) also provide an efficient description of the observed rotation curves (Sanders 1996). Early studies by e.g. Kalnajs (1983) claimed that, based on the optical rotation curves that were used, there was no need to invoke DM within the optical radius for some galaxies. Hɪ observations, however, showed a dramatically different picture (Bosma 1978, Begeman 1987). Substantial amounts of DM were needed to describe the observed flat rotation curves outside the optical disk.

Measurements of the distribution of the DM must be extracted from the rotation curve. This is usually done by computing the rotation curves of the visible matter and subtracting these from the observed total rotation curve. The residuals show the dynamical signature of DM. This procedure typically has the following free parameters: a length scale and density for the halo and a mass-to-light ratio $(M/L)_\star$

of the stellar component. A major problem is that the value of $(M/L)_\star$ is not known *a priori*, and may differ from galaxy to galaxy. Many different values of $(M/L)_\star$, and therefore many combinations of halo parameters, yield equally good descriptions of the data (van Albada et al. 1985). It is for many galaxies possible to make a good fit to the rotation curve by completely ignoring the contribution of the stellar disk, even though it obviously plays an important role in the inner parts of many galaxies. Without additional knowledge to constrain $(M/L)_\star$ (e.g. information about vertical stellar velocity dispersion or derived from stellar population synthesis models) it is not possible to unambiguously determine its value. Goodness-of-fit estimators are sensitive to small variations and uncertainties in the data (even when the data is of superior quality) (Lake & Feinswog 1989) and are thus less suited for simultaneously determining *all* free parameters in a fit. The mathematically "best" fit is therefore not always the physically most meaningful one.

Using the observation that the rotation curves derived for the stellar components of HSB galaxies can usually be scaled so that they almost completely describe the observed total rotation curves in the optical disks of these HSB galaxies (e.g. Kent 1986), van Albada & Sancisi (1986) introduced the maximum-disk hypothesis. This hypothesis reduces the

number of free parameters in rotation curve fits by maximizing the contribution of the stellar disk [i.e. $(M/L)_\star$] and thus minimizing the amount of DM invoked to explain the observed rotation curves.

It is still unclear whether the maximum disk hypothesis is a realistic one. For some HSB galaxies stellar population synthesis models yield values of $(M/L)_\star$ that are consistent with the maximum disk measurements (van Albada & Sancisi 1986). The presence of disk features such as spiral arms or bars argues for a high $(M/L)_\star$ (Athanassoula, Bosma & Papaioannou 1987). Kuijken & Gilmore (1989) showed, however, that there is only enough matter in the disk of our Galaxy for it to be about half-maximum disk. Measurements of the stellar velocity dispersions in HSB galaxies (Bottema 1995) show that maximum disk may overestimate the amount of matter present in the disk by some 60 per cent.

As the maximum disk hypothesis gives for each galaxy the *maximum* possible $(M/L)_\star$, any conclusions about structural parameters of halos are only "lower limits." Nevertheless, attempts have been made to find systematic relations between the observable properties of spiral galaxies and their dark halo properties.

A general conclusion is that the importance of DM increases towards later types (Persic & Salluci 1991). Coupled with the finding that the surface brightness also decreases towards later types (de Jong 1995), this means that low surface brightness (LSB) galaxies are a prime example of galaxies that are extremely interesting for deriving structural properties of DM halos.

These galaxies are very late-type spirals with central surface brightnesses much lower than those of "classical" late-type HSB galaxies (de Blok, McGaugh & van der Hulst 1996 [hereafter BMH96], Zwaan et al. 1995, van der Hulst et al. 1993; see also the reviews by Impy & Bothun 1997 and Bothun, Impey & McGaugh 1997). Their blue colors (de Blok, van der Hulst & Bothun 1995, McGaugh & Bothun 1994, Rönnback & Bergvall 1994), low star formation rates (McGaugh 1992, van der Hulst et al. 1993, van den Hoek et al. 1997), low oxygen abundances (McGaugh 1994, Rönnback & Bergvall 1995) and high gas-fractions (BMH96, McGaugh & de Blok 1997), all give rise to the picture that these galaxies are slowly evolving and still in an early evolutionary state.

Recently a number of rotation curves of LSB galaxies have been measured (BMH96). A preliminary investigation showed a systematic trend of increasing total mass-to-light ratio within a number of scale lengths with decreasing surface brightness, from values of ~ 1 for HSB galaxies to ~ 10 for the dimmest measured LSB galaxies (Fig. 13 in BMH96), consistent with predictions made using the Tully-Fisher relation (Zwaan et al. 1995). The increasing importance of DM makes an investigation into the halo parameters extra interesting as the parameters will depend less strongly on assumed values of $(M/L)_\star$, and one can therefore be quite sure that the derived parameters are indeed close to the intrinsic parameters of the halo.

A comparison of a HSB and a LSB galaxy at identical positions on the Tully-Fisher relation (i.e. at fixed $V_{\max}$) (de Blok & McGaugh 1996) showed that LSB galaxy UGC 128 is almost a factor 10 less dense than the HSB galaxy NGC 2403 (analogous with their low stellar and HI surface densities).

UGC 128 also has a factor of 7 higher total M/L (measured within a fixed number of scale lengths) and must therefore be more massive than HSB galaxy NGC 2403 (which has the same luminosity).

In this paper we will discuss disk-halo decompositions of the sample of LSB galaxies from BMH96 and compare the structural parameters of the dark and luminous mass components of HSB and LSB galaxies. In Section 2 we describe the sample; Section 3 covers various aspects of the effects on resolution and beam-smearing on the rotation curves. In Section 4 the actual decompositions are presented, while in Section 5 we discuss the results and compare them with what is known about other galaxies. In Section 6 the systematic relations between the masses of the different components (gas, stellar, dark) are discussed, while in Section 7 we discuss the trends of volume and surface density as a function of surface brightness. In Section 8 our main results are summarized. In Appendix A a summary of the Bottema disk (Sect. 4.4) is given.

2   THE LSB SAMPLE

We refer to BMH96 for an extensive sample description. We have supplemented that sample with the rotation curves of an additional 5 LSB galaxies as presented in van der Hulst et al. 1993. The rotation curves in general have maximum rotation velocities between 50 and 120 km s^{-1}, and rise more slowly than HSB curves with similar maximum velocity. Only a few of the rotation curves show clear signs of flattening towards the outermost radii. Optical properties of the sample are presented in McGaugh & Bothun (1994), de Blok et al. (1995), and van der Hulst et al. (1993). The properties of the sample galaxies are summarized in the top panel of Table 1. We adopt a Hubble constant of 75 km s^{-1} Mpc^{-1}.

As described in BMH96 the rotation curves were derived from major-axis position-velocity diagrams. Inclinations were determined from a comparison of optical, HI and kinematical inclinations. The position angle and inclination were both kept fixed during the derivation of the curves. Inspection of the position-velocity diagrams in Fig. 2 of BMH96 shows that not all rotation curves are well suited for a disk-halo analysis. A number of observations clearly suffer from low resolution or low inclination.

In order to select only those galaxies where a disk-halo decomposition is a sensible exercise, we restricted the sample by rejecting those galaxies that did not meet one of the following criteria:

  (i) inclination $i > 25°$,
 (ii) radius $R > 2$ beams,
(iii) asymmetries between approaching and receding sides of rotation curves < 10 km s^{-1}.

This resulted in the rejection of seven galaxies. These are listed in Table 2 with the reason for rejection.

The choice for a 25 degree cut-off may seem a rather liberal choice, which in a sense we are forced to apply due to the selection biases against high-inclination LSB galaxies (Davies 1990, Schombert et al. 1992, Dalcanton & Shectman 1996). An analysis of the scatter in the LSB TF relation presented in Zwaan et al. (1995) does show however that

Table 1. Properties of LSB and HSB samples

Name	D (Mpc)	$\mu_0(B)$ (mag/")	h (kpc)	$B - V$ (mag)	$M_{abs}(B)$ (mag)	R_{25} (kpc)	R_{max} (kpc)	V_{max} (km s^{-1})
LSB sample (this work)								
F561-1	63	23.3	3.6	0.55	-17.8	6.4	10.1	52
F563-1	45	23.6	2.8	0.64	-17.3	5.0	17.7	111
F563-V1	51	24.3	2.4	0.59	-16.3	3.2	7.4	30
F563-V2	61	22.1	2.1	0.51	-18.2	6.8	9.2	111
F564-V3	6	24.1	0.4	0.56	-11.1	0.3	$\sim$2	$\sim$40
F565-V2	48	24.7	2.7	0.51	-15.4	2.3	8.4	51
F567-2	75	24.4	5.7	0.61	-17.4	3.2	11.3	64
F568-1	85	23.8	5.3	0.58	-18.1	7.4	14.9	119
F568-3	77	23.1	4.0	0.61	-18.3	7.9	16.5	120
F568-V1	80	23.3	3.2	0.57	-17.9	6.2	19.0	124
F571-8	48	23.9^{a,c}	5.2^c	*	-17.6^a	7.7	15.6	133
F571-V1	79	24.0	3.2	0.55	-17.0	3.8	14.6	73
F571-V2	16	*	*	*	*	*	3.7	45
F574-1	96	23.3^a	4.3	*	-18.4^a	17.7	15.4	100
F574-2	88	24.4	6.0	0.59	-17.6	3.8	10.7	40
F577-V1	80	24.0	4.3	0.40	-18.2	6.6	8.9	30
F579-V1	85	22.8^a	5.1	*	-18.8^a	11.1	17.3	100
F583-1	32	24.1	1.6	*	-16.5	3.3	14.6	85
F583-4	49	23.8^a	2.7	*	-16.9^a	6.4	10.0	67
U0128	60	24.2	6.8	0.60	-18.8	9.0	42.3	131
U1230	51	23.3	4.5	0.47	-18.3	5.2	34.7	102
U5005	52	23.8^a	4.4	*	-17.8^a	10.4	27.8	99
U5750	56	23.5^a	5.6	*	-18.7^a	9.5	21.8	75
U5999	45	23.5^a	4.3	*	-17.6^a	9.8	15.3	155
"HSB" sample (Broeils 1992)								
DDO154	4	23.2	0.5	0.29	-13.8	1.0	7.6	48
DDO168	3.5	23.4	0.9	0.22	-15.2	1.7	3.4	55
DDO170	12	*	1.3	*	-14.5	2.5	9.6	66
N55	1.6	21.3	1.6	0.38	-18.6	8.9	10.2	87
N247	2.5	23.4	2.9	0.45	-18.0	7.3	9.9	108
N300	1.8	22.2	2.1	0.56	-17.8	5.1	10.6	97
N801	79.2	21.9	12	0.66	-21.7	36.4	58.7	222
N1003	11.8	21.7	1.9	0.40	-19.2	9.2	31.3	115
N1560	3	23.2	1.3	0.43	-15.9	4.3	8.3	79
N2403	3.3	21.4^b	2.1	0.38	-19.3	8.4	19.5	136
N2841	18	21.1^b	4.6	0.80	-21.7	22.6	81.1	323
N2903	6.4	20.5^b	2.0	0.59	-21.0	11.7	24.2	201
N2998	67.4	20.3	5.4	0.48	-21.9	28.2	46.6	214
N3109	1.7	23.2	1.6	*	-16.8	4.3	8.2	67
N3198	9.4	21.6^b	2.6	0.46	-19.4	11.4	29.9	157
N5033	11.9	23.0^b	5.8	0.48	-20.2	18.3	35.4	222
N5533	55.8	23.0	11.4	0.80	-21.4	26.2	74.4	273
N5585	6.2	21.9	1.4	0.42	-17.5	4.7	9.6	92
N6503	5.9	21.9	1.7	0.56	-18.7	5.4	22.2	121
N6674	49.3	22.5	8.3	0.61	-21.6	29.8	64.5	266
N7331	14.9	21.5^b	4.5	0.70	-21.4	23.4	36.7	241
U2259	9.8	22.3^b	1.3	*	-17.0	3.7	7.6	90
U2885	78.7	22.0^b	13	*	-22.8	62.8	72.5	298

a: converted from R-band measurement
b: derived from r-band profiles, converted using $B = r + 1$ (Kent 1986)
c: μ_0(face on) of F571-8 was computed assuming μ(face on) $=$ $(z_0/h)\mu$(edge on) (i.e. optically thin). h(face on) was found to be $\sim$ 1.4h(edge on) following method of Peletier et al. (1995).

Table 2. Rejected galaxies

Name	Limitation
F561-1	$R < 2$ beams; $i < 25°$
F563-V1	$R < 2$ beams; gross asymmetry
F564-V3	$R < 2$ beams; low S/N
F567-2	gross asymmetry; $i < 25°$
F574-2	$R < 2$ beams; $V(R)$ steeply rising
F577-V1	$R < 2$ beams; gross asymmetry
F579-V1	gross asymmetry

this scatter does not increase significantly when increasingly lower-inclination galaxies are included until a value of 25 degrees.

The effects of lower resolution are more difficult to model, and will be described extensively in the next section.

3 BEAM-SMEARING

Early high-resolution studies of spiral galaxy kinematics using synthesis radio telescopes did mostly target galaxies with large angular sizes (e.g. Bosma 1978, Begeman 1987, Broeils 1992). The rotation curves of these galaxies are in general well-determined. Unfortunately there are only a limited number of galaxies in the sky that have suitably large angular sizes for such detailed investigations. Galaxies with smaller apparent sizes (because of smaller intrinsic sizes and/or larger distances) can only be observed at a smaller linear resolution.

A side-effect of this lower resolution is that the line profiles will be artificially broadened and any sudden change in the velocity gradient within the beam will be smoothed out. The observed change in the velocity gradient will thus appear to be smaller and the rotation curve will appear to rise less steeply. This effect is called "beam smearing."

Bosma (1978) investigated the behavior of a steeply rising model rotation curve at different resolutions. He showed that if the ratio between the Holmberg radius of a galaxy and the half power beam width is smaller than ~ 7 to ~ 10, beam smearing can have serious effects on the steep inner parts of the curve. Rubin et al. (1989) make the point that if one wants to decompose the mass distribution of a galaxy into its disk and halo components one needs rotation curves of high accuracy in their inner portions, as "the maximum mass which can reside in the disk is constrained principally by the inner rise of the rotation curve." This statement is based on investigations into a sample of primarily steeply rising rotation curves, but remains true also for slowly rising rotation curves, although, as we will show, to a much lesser extent.

The rotation curves of LSB galaxies presented in BMH96 are not high-resolution rotation curves and beam smearing is a potential problem. The decrease in the slope of the rotation curves would disguise potentially steep rotation curves as gently rising solid-body curves. Here we will present some arguments why this effect is not significant in the BMH96 data, implying that the rotation curves of LSB galaxies are truly slowly rising.

3.1 Evidence from BMH96

The most direct evidence why beam smearing effects do not dominate the data from BMH96 comes from that data itself. If the data were severely affected by resolution effects, one would not expect to observe steeply rising rotation curves.

Figure 1 shows the major-axis position-velocity diagrams of LSB galaxies F579-V1 and F568-1. Both galaxies are at similar distances (77 *vs* 85 Mpc, a difference of less than 10 per cent); both were observed with the same telescope with identical beam sizes; both have an inclination of 26 degrees, a comparable HI distribution and almost identical scale lengths. The effects of beam smearing are effectively identical in both galaxies.

It is clear that the rotation curve of F579-V1 rises much more steeply than that of F568-1. The fact that we *do* observe a steeply rising rotation curve in F579-V1, shows that the approximately solid body rotation observed in F568-1 is not caused by beam-smearing. This makes it unlikely that the solid-body rotation observed in other LSB galaxies from BMH96 is caused by observational effects. It should be noted that the solid-body rotation is also seen in those LSB galaxies observed at higher resolutions (e.g. F563-1 and F583-1) and is in general found in other high resolution observations of very late-type galaxies (see e.g. IC 2574 in Martimbeau, Carignan & Roy 1994).

3.2 Modeling beam smearing

Another way to quantify the effects of beam smearing is to construct model galaxies with known properties and "observe" these at increasingly lower resolutions. As beam smearing affects the full two-dimensional velocity field of a galaxy, it is necessary to construct complete model data cubes, smooth these to lower resolutions using a Gaussian beam and then construct velocity fields and derive rotation curves.

3.2.1 Constructing models

We constructed a number of model data cubes using the task GALMOD in the Groningen Image Processing System GIPSY. This program distributes "HI clouds" in a specified data cube using an input radial HI distribution and rotation curve as distribution functions. The galaxy can be given any inclination or position angle. This model can then be "observed" at any desired spatial and velocity resolution. For simplicity we adopted a uniform, constant density HI distribution for all models. We could have used any HI distribution, but decided to opt for the simplest distribution to isolate the effects of beam smearing.

The magnitude of the beam smearing effects also depends on inclination. At high inclinations the beam will cover a larger part of the velocity field off the major axis than at lower inclination, thus "diluting" the major axis rotation velocity. For a fixed beam size the effects of beam smearing will still depend on inclination, with the worst effects occuring in the highest-inclination galaxies.

In order to mimic the BMH96 observations, we chose an inclination of 40 degrees for our model galaxies, equal to the average inclination of the 12 "F"-galaxies in BMH96. To cover the full range of known rotation curve shapes we
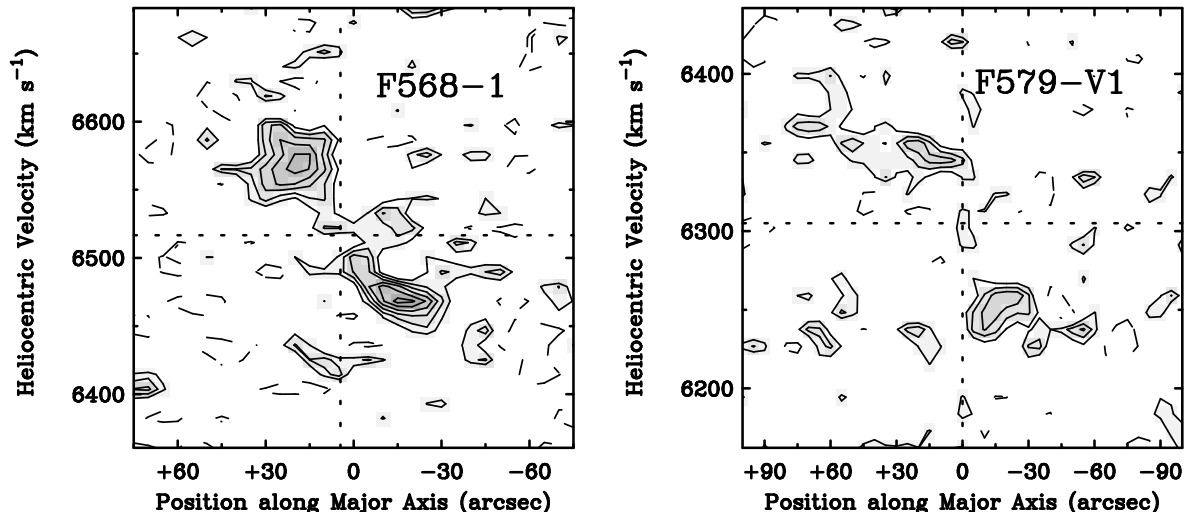
Figure 1. Major-axis position velocity diagrams of LSB galaxies F568-1 and F579-V1. Both galaxies are at approximately the same distance, have identical inclinations and were observed with the same telescope with identical beam sizes. It is clear that the rotation velocity in the inner parts of F579-V1 increases more rapidly than in F568-1. If these observations suffered from heavy beam-smearing this difference could never have been observed. Contour levels are -2σ (dashed contours) and 2,4,6,.. σ contours (full contours).

adopted three different input rotation curves. These are shown in Fig. 2. Radii and velocities are all expressed as fractions of the maximum radius and velocity of the input models R_{max} and V_{max}. These were identical for all three models.

The first model has a constant rotation velocity at all radii, and is the perfect example of a flat rotation curve. This is an extreme, but not unrealistic representation of the steeply rising rotation curves found in early-type HSB galaxies (e.g. UGC 2885 or NGC 2841 in the compilation by Rhee 1996).

The second curve is a simplified version of that presented in Fall & Efstathiou (1980):

$$V(r) = V_{max}\sqrt{\frac{r^2}{r^2 + d^2}}.$$

The constant d was given a value of $0.2R_{max}$. This model rotation curve (which we will refer to as the "FE curve") resembles that of a normal late-type galaxy (see e.g. the high resolution rotation curves of NGC 1560, NGC 3198 or NGC 2403 in Rhee 1996).

The third curve is another extreme case: pure solid body rotation with a still increasing rotation velocity at R_{max}. This solid-body rotation *is* found in dwarf galaxies (see e.g. the well defined high resolution curve of IC 2574 in Martimbeau et al. 1994 or NGC 3109 from Rhee 1996).

The full three-dimensional high-resolution model data cubes constructed using these curves, were each smoothed with Gaussian beams with FWHM sizes of $(1/10, 1/8, 1/6, 1/4, 1/2) \times R_{max}$. This obviously resulted for each of the three cases in data cubes where the *radius* of the disk measured 10, 8, 6, 4 and 2 beams respectively. Velocity fields were constructed from these cubes using the GIPSY task

MOMENTS. Analogous to the procedure outlined in BMH96, the rotation curves of each of the smoothed data cubes were determined from major-axis position-velocity diagrams.

As noted before, all models were computed assuming model galaxy inclinations of 40 degrees. The original and smoothed de-projected curves are presented in Fig. 2. A first glance shows that indeed the effects of beam smearing are most severe for the flat rotation curve which has the steepest inner "slope." The beam smearing effects are negligible in the solid body curve, where the only effect is an apparent flattening at the outermost radii. The FE curve retains its shape and slope down to a resolution of 4 beams. The input and output curves only start to differ significantly at resolutions of 2 beams.

3.2.2 Comparison with observations

We now compare the smoothed models with some of the observations from BMH96. We will use the rotation curves of F568-3 and F568-V1. These galaxies both have inclinations of 40 degrees and are thus directly comparable with the model curves. Both curves have a resolution of slightly less than 4 beams and should thus be compared to the 4-beam models, as is done in Fig. 3. The observed curves were scaled using the R_{max} and V_{max} given in BMH96.

It is clear that the observed curves are best matched by the FE curve, although a completely solid body curve cannot be ruled out at 4 beams resolution. The only way the observations can be reconciled with a rotation curves that are flat down to a small radius, is at a resolution of 2 beams, that is, a factor of 2 worse than the present observations. At a resolution of 4 beams a flat curve can be ruled out.

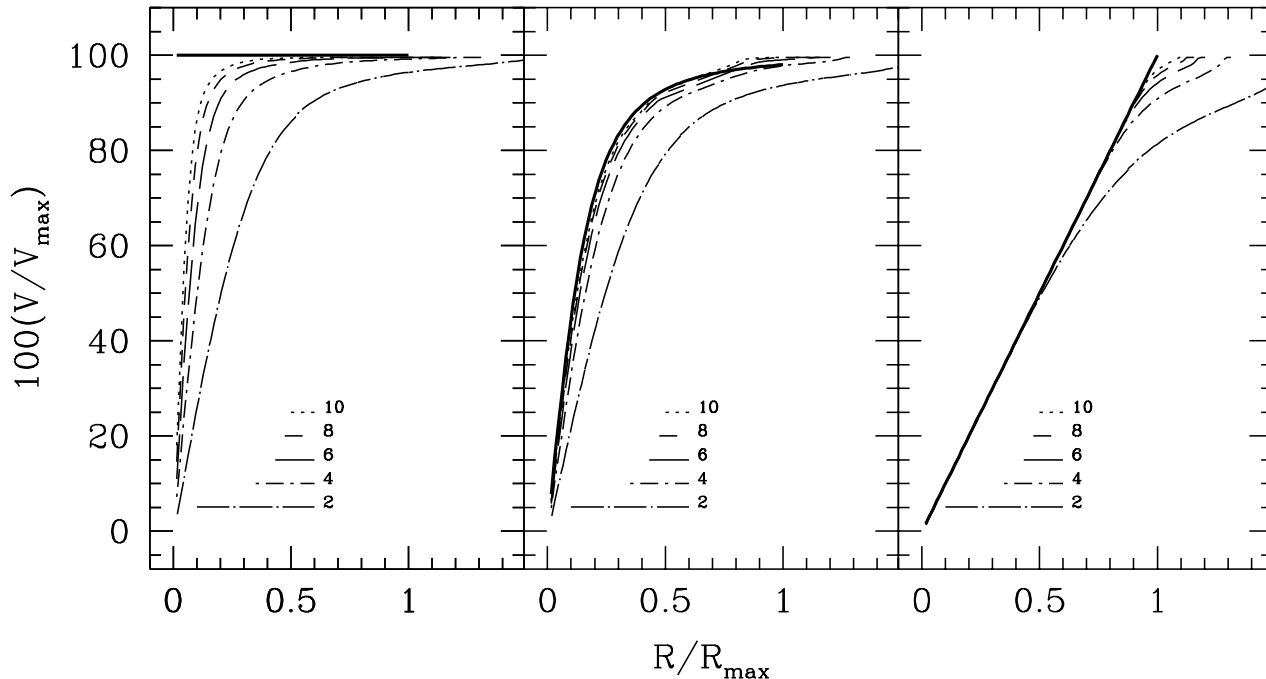The question that remains to be answered then, is how

Figure 2. Model rotation curves illustrating the effects of beam-smearing. The heavy lines show the input rotation curves: flat (left panel), late-type-like (center), and solid-body (right). The beam-smeared versions of these curves are shown as the dashed and dotted lines. These lower resolution curves were derived using the full 3-dimensional data cubes. The resolution expressed in beams is 10 (dotted), 8 (short dash), 6 (long dash), 4 (short dash-dot) and 2 (long dash-dot). It is clear that the effects of beam-smearing are most severe in the flat case (left panel), while the effects of beam-smearing are only small in the inner parts of the late-type and solid-body curves. In the latter two cases the shape of the curves do not change dramatically down to a resolution of 2 beams. The small bump visible in the FE-curves at $R \simeq 1$ is caused by the limited velocity resolution used in the models, in order to mimic the BMH96 observations.

likely it is that LSB galaxies have FE-like rotation curves. First, as is shown by the studies of Casertano & van Gorkom (1989) and Broeils (1992) of high resolution H I rotation curves, *only* those galaxies with maximum rotation velocities of more than 180 km s^{-1} ($M_B \leq -19$) have steep inner rotation curves. The steep inner curves are usually interpreted as the dynamical signature of a strong bulge component. Galaxies that rotate slower have gradually rising rotation curves, resembling the FE model curve. The LSB galaxies from BMH96 have maximum rotation velocities between 50 and 120 km s^{-1}, luminosities M_B between -16 and -18, and have only the faintest trace of a central condensation. So, *if* LSB galaxies are late-type galaxies, as all of the available evidence suggests, then it is not surprising that they have slowly rising rotation curves.

This is supported by work from Coradi & Capaciollo (1990) who measured the inner slopes of *optical* rotation curves of 139 galaxies of a large range of Hubble types and luminosities. They found a strong correlation between the magnitude of this slope, Hubble type and luminosity: 75 per cent of the galaxies in their sample with luminosities $19 < M_B \leq -18$ have slowly rising, non-flat rotation curves[*], while all of the galaxies fainter than -18 have

slowly rising rotation curves. The result holds for the relation with Hubble types: 80 per cent of the galaxies with Hubble type Sd and later have slowly rising rotation curves.

3.3   Evidence from NGC1560

As LSB galaxies are late-type galaxies, a third possibility to investigate the effects of beam-smearing is by taking a high-resolution observation of a late-type galaxy and smooth it to lower resolution. We have selected NGC 1560 for this purpose. This galaxy is a LSB dwarf galaxy ($\mu_0(B) = 23.2$ mag arcsec^{-2}, for other properties see Table 1), for which a high-resolution rotation curve is available (Broeils 1992). This curve is shown in the left panel of Fig. 4. The beam size for this WSRT observation was $13'' \times 14''$, and the extent of the rotation curve is 38 beams. Combined with the small distance of only 3 Mpc, we can be that sure beam-smearing is of no importance in this observation.

We have used one-dimensional smoothing with a Gaussian filter to bring the total rotation curve and those of the

consistent with these results. F579-V1 is the most luminous galaxy in the "F"-sample from BMH96, and in fact falls in the $19 < M_B \leq -18$ category.

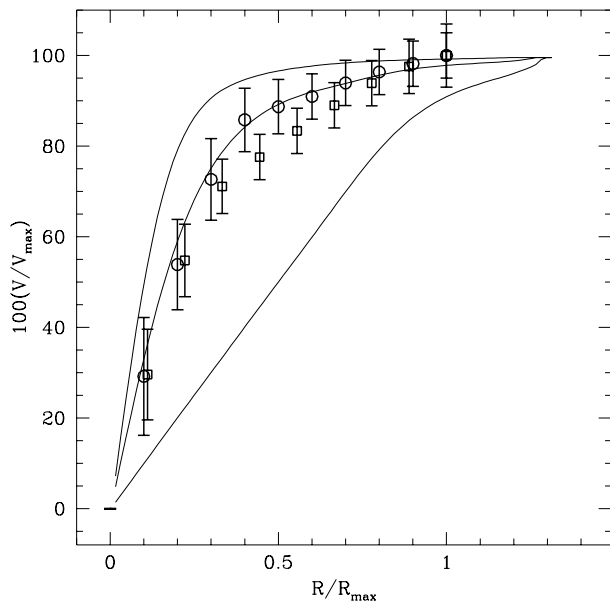[*] Note that the steep slope of the F579-V1 rotation curve is

Figure 3. Comparison of the model rotation curves with observed curves. The three light lines show, from top to bottom, the rotation curves of the flat model, the FE model and the solid-body model at a resolution of 4 beams. Super imposed are the rotation curves of F568-V1 (squares) and F568-3 (circles). The latter curves are consistent with the FE-model, although the shapes suggest that a slightly steeper solid-body model is also possible. The flat model can be excluded.

stars and gas to lower resolutions. As the effects of one-dimensional smoothing of the rotation curve are less severe than full two-dimensional smoothing of the velocity field, we have smoothed the curves to a resolution of 3 beams. We found by trial and error that this corresponds most closely to a full two-dimensional smoothing with a resolution of 4 beams.

The smoothed curve is shown in the right panel of Fig. 4. The other curves shown in the figure will be discussed in Section 5.1. A comparison of the high- and low-resolution curves shows that the only effects this beam smearing exercise has had on the curves is a loss of detail. The shapes and amplitudes of the curves have remained unchanged. This again shows that slowly rising rotation curves can be studied at much lower resolutions than rapidly rising ones without a dramatic loss of information. We conclude that the rotation curves of the LSB galaxies are intrinsically slowly rising. Beam smearing effects do not dominate the BMH96 data.

4 DISK HALO DECOMPOSITION

We now return to the disk-halo decompositions and subsequent mass modeling. Before giving the results of the decompositions, we first describe the mass components used.

Stellar disk For the stellar disk the B and R-band photometry presented in de Blok et al. (1995), and McGaugh & Bothun (1994) was used. The rotation curve of the disk was computed following Casertano (1983) and Begeman (1987). The disk was assumed to have a vertical sech-squared dis-

tribution with a scale height $z_0 = h/6$ (van der Kruit & Searle 1981). The exact value of z_0 does not influence the amplitude and shape of the rotation curve to any significant degree. No bulge component was included as there is no evidence that bulges contribute significantly to the mass distribution in most LSB galaxies (see de Blok et al. 1995, McGaugh, Bothun & Schombert 1995). Prior to the decomposition the light distribution curves were resampled to the H I resolution.

Isothermal dark halo We assume a spherical pseudo-isothermal halo with a density profile

$$\rho(R) = \rho_0 \left[1 + \left(\frac{R}{R_C} \right)^2 \right]^{-1}, \tag{1}$$

where ρ_0 is the central density of the halo, and R_C the core radius of the halo. This density profile results in the rotation curve

$$V_{\text{halo}}(R) = \sqrt{4\pi G \rho_0 R_C^2 \left[1 - \frac{R_C}{R} \arctan\left(\frac{R}{R_C} \right) \right]}. \tag{2}$$

The asymptotic velocity of the halo, V_∞, is given by

$$V_\infty = \sqrt{4\pi G \rho_0 R_C^2}. \tag{3}$$

To characterize this halo only two out of the three parameters (ρ_0, R_C, V_∞) are needed, as equation (3) determines the value of the third parameter. The mass of the halo integrated out to radius r is

$$M_{\text{d}}(r) = \frac{V_{\text{halo}}^2 r}{G} = 4\pi \rho_0 R_C^2 \left[r - R_C \arctan\left(\frac{r}{R_C} \right) \right]. \tag{4}$$

Because $(M/L)_\star$ is unknown we present disk-halo decompositions using three different assumptions for $(M/L)_\star$:

(i) maximum disk (Sec. 4.2),
(ii) minimum disk (Sec. 4.3), and
(iii) "Bottema disk" (Sec. 4.4).

Each of the rotation curves was fitted using a program which determines the best-fitting combination of R_C, V_∞, $(M/L)_\star$, using a least squares fitting. Any combination of these three parameters could be fit, or kept fixed at some initial value. The program uses as input the rotation curve of the gas, the total measured rotation curve, and the rotation curve of the stellar disk computed from the observed light distribution (i.e. with an $(M/L)_\star = 1$) (see Begeman 1987).

4.1 HSB and LSB samples

We will compare the properties of our LSB galaxies with those of mostly HSB galaxies with well-defined H I rotation curves. The latter have been taken from the compilation by Broeils (1992) and references therein. This "HSB sample" does not consist of just disks obeying Freeman's Law (i.e. galaxies with $\mu_0 \simeq 21.6B$-mag arcsec^{-2}) (Freeman 1970): a large range of central surface brightnesses is found, from Freeman disks to galaxies with surface brightnesses approaching those of the LSB galaxies. The mean surface brightness of the HSB sample ($\langle\mu_0\rangle = 22.2$) is still 1.5 magnitudes brighter than that of the LSB sample ($\langle\mu_0\rangle = 23.7$). Comparing the two samples gives a good impression of the change in properties of spiral galaxies over a large range in surface brightness. Properties of the HSB sample are given in the bottom panel of Table 1.

Table 3. Disk and halo parameters LSB galaxies

	Maximum disk R-band						Maximum disk B-band					
Name	$\left(\frac{M}{L}\right)_\star$	R_C	V_∞	ρ_0	$M_\star$	$M_{\rm d}$	$\left(\frac{M}{L}\right)_\star$	R_C	V_∞	ρ_0	$M_\star$	$M_{\rm d}$
(1)	(2)	(3)	(4)	(5)	(6)	(7)	(8)	(9)	(10)	(11)	(12)	(13)
F563-1	6.3	3.6	109.0	17.2	0.962	3.529	9.0	4.7	106.8	9.6	1.374	3.063
F563-V2	*	*	*	*	*	*	2.7	3.8	115.2	17.2	0.658	1.456
F565-V2	3.1	4.6	61.8	3.4	0.103	0.310	3.6	5.6	70.7	2.9	0.097	0.331
F568-1	2.0	2.6	126.4	43.7	0.394	4.163	3.0	2.6	124.3	40.8	0.587	3.993
F568-3	1.8	5.4	136.5	11.8	0.429	4.190	2.6	6.6	147.4	9.1	0.532	4.305
F568-V1	2.0	3.8	135.9	23.6	0.207	5.929	2.6	4.2	137.2	19.5	0.332	5.824
F571-8	0.3^a	7.9	249.9	18.2	0.097	9.934	*	*	*	*	*	*
F571-V1	3.0	4.4	78.3	5.9	0.253	1.279	3.7	5.5	86.5	4.6	0.228	1.379
F574-1	0.9	10.2	172.1	5.3	0.216	3.681	*	*	*	*	*	*
F583-1	1.5	3.4	97.8	15.5	0.045	2.236	*	*	*	*	*	*
F583-4	0.9	6.0	104.2	5.6	0.065	0.962	*	*	*	*	*	*
U0128	3.0	6.4	136.3	8.3	1.043	14.32	4.0	6.7	125.9	6.6	2.254	12.120
U1230	0.7	4.5	102.7	9.5	0.187	6.912	1.0	5.1	100.8	7.2	0.457	6.48
U5005	4.5	3.2	91.8	15.0	0.675	4.467	*	*	*	*	*	*
U5750	0.7	4.5	83.4	6.4	0.086	2.526	*	*	*	*	*	*
U5999	3.0	4.6	190.7	32.0	0.444	7.966	*	*	*	*	*	*

	Minimum disk						Bottema disk, B-band				
Name	$M_{\rm g}$	R_C	V_∞	ρ_0	$M_{\rm d}$		$\left(\frac{M}{L}\right)_\star$	R_C	V_∞	ρ_0	$M_{\rm d}$	$M_\star$
(14)	(15)	(16)	(17)	(18)	(19)		(20)	(21)	(22)	(23)	(24)	(25)
F563-1	0.385	1.5	118.6	111.2	5.042		1.7	1.8	113.4	75.4	4.507	0.203
F563-V2	0.321	1.9	127.6	80.9	2.479		1.3	2.8	118.9	34.4	1.858	0.365
F565-V2	0.084	2.8	59.1	8.4	0.399		1.3	3.4	59.1	5.6	0.355	0.038
F568-1	0.557	2.0	130.0	82.2	4.731		1.5	2.6	128.6	45.4	4.313	0.246
F568-3	0.394	3.4	131.2	28.2	4.742		1.6	5.2	135.7	12.5	4.219	0.308
F568-V1	0.344	3.1	134.3	35.0	6.153		1.4	3.7	135.5	25.5	5.972	0.128
F571-8	0.202	7.0	235.3	21.0	9.725		*	*	*	*	*	*
F571-V1	0.164	2.5	79.9	18.6	1.640		1.4	3.3	78.2	10.7	1.448	0.103
F571-V2	0.016	0.8	51.1	75.5	0.156		*	*	*	*	*	*
F574-1	0.485	7.5	150.6	7.5	3.704		1.5	12.6	188.9	4.1	3.502	0.284
F583-1	0.243	2.8	96.5	21.8	2.322		1.5	3.4	97.9	15.3	2.235	0.036
F583-4	0.077	4.7	96.4	7.8	1.008		1.5	7.4	112.3	4.3	0.905	0.085
U0128	0.882	4.0	137.7	21.7	16.020		1.5	5.2	135.7	12.7	14.90	0.444
U1230	0.812	3.7	103.4	14.2	7.275		1.1	5.8	104.1	6.0	6.697	0.294
U5005	0.406	2.2	102.9	40.1	6.034		1.5	2.4	97.2	31.4	5.337	0.182
U5750	0.140	4.0	87.6	9.1	2.900		1.5	5.5	84.2	4.3	2.386	0.146
U5999	0.252	4.1	192.1	40.8	8.520		1.5	4.3	191.0	36.0	8.209	0.175

Note: $(M/L)_\star$ is in units of $(M_\odot/L_\odot)$ in the respective bands; R_C is in units of kpc, V_∞ in units of km s^{-1}, ρ_0 is in units of $10^{-3}\ M_\odot {\rm pc}^{-3}$; all masses are in units of $10^{10} M_\odot$.
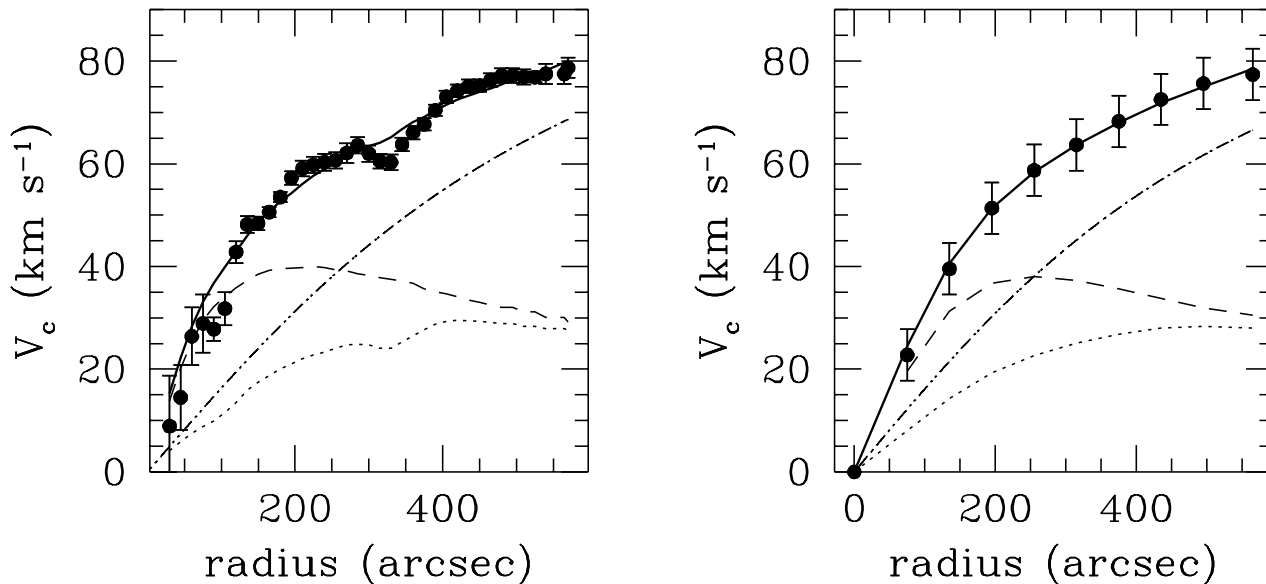a: $(M/L)_{\rm bulge} = 0$

Figure 4. High and low resolution rotation curves of NGC 1560. The left panel shows the original high resolution observation from Broeils (1992). The curves measures 38 beams, and is well-resolved. The right panel shows the same data but smoothed to a resolution of only 3 beams. It is striking that the overall shape and amplitude of the curves have remained virtually unchanged. This is discussed more fully in Section 3.3. The dashed and dotted lines show the maximum disk decompositions for both cases. The dotted lines represent the rotation curve of the gas component, the dashed lines the rotation curve of the maximum stellar disk. The dash-dotted lines are the rotation curves of the halos as derived from this decomposition. There is almost no difference between the low- and high-resolution halo parameters. This is discussed more fully in Section 5.1. The fitting parameters are given in Table 6.

4.2 Maximum disk fits

The maximum disk hypothesis attributes as much of the observed rotation velocity to the stellar disk as possible. It therefore always yields an upper limit to the $(M/L)_\star$ in a galaxy. For HSB galaxies the maximum disk hypothesis can explain almost all of the observed rotation velocity in the inner parts with just the stellar disk. For LSB galaxies the situation is quite different. Figure 5 shows the maximum disk decompositions of their rotation curves. The resulting disk and halo parameters are summarized in Table 2, together with the masses of the various components, as measured within the outermost radius $R_{\max}$ of the rotation curve (Table 1). For those galaxies where both R and B photometry were available we have done separate decompositions for both bands, which are compared in Fig. 6. The core radii and asymptotic velocities correspond very well to each other in both sets, as do the maximum disk $(M/L)_\star$ ratios when the $B - R$ colors of the galaxies are taken into account. To compare those LSB galaxies for which only R-band data is available with B-band literature data, we will convert the measured maximum disk $(M/L_R)_\star$ ratios to B-band values assuming an average $B-R$ color of 0.88 (de Blok et al. 1995, cf. Fig. 6). Our results do not depend on this conversion as the halo is the most dominant component and its parameters are therefore not very sensitive to the precise value of $(M/L)_\star$. The maximum disk decompositions for the HSB samples have been taken from Broeils (1992) and are for convenience summarized in Table 4.

4.3 Minimum disk

Many of the rotation curves of LSB galaxies are best fitted by a minimum disk, that is, under the assumption that $(M/L)_\star = 0$. We have calculated the halo parameters under this assumption (Table 3). We will compare them with the maximum disk parameters in Section 5.4, but already note that there is little change in the structural parameters of the halos, due to the DM dominance. Although minimum disk is not a realistic assumption for HSB galaxies, we have for comparison also made minimum disk fits to the rotation curves of the HSB sample (Table 5). Not all galaxies could be fitted: especially the earlier types (with bulges) have rotation curves that rise too steeply to be fitted by a simple isothermal model with a finite core radius, thus clearly showing the need for a compact luminous component.

4.4 Bottema disk

Bottema (1995) has measured the stellar velocity dispersions of a sample of HSB spiral galaxies and found that the dispersion is related to the maximum rotation velocity. For a Freeman disk with a color $B - V = 0.7$ he derived $(M/L_B)_\star \simeq 1.8$. The stellar disks of the galaxies in his sample supply approximately 63% of the total measured velocity at $2.2h$ (where the rotation curve of an exponential disk peaks). These results were derived under the explicit assumption of Freeman's Law (which holds for most of Bottema's galaxies). It is obvious that Bottema's orig-
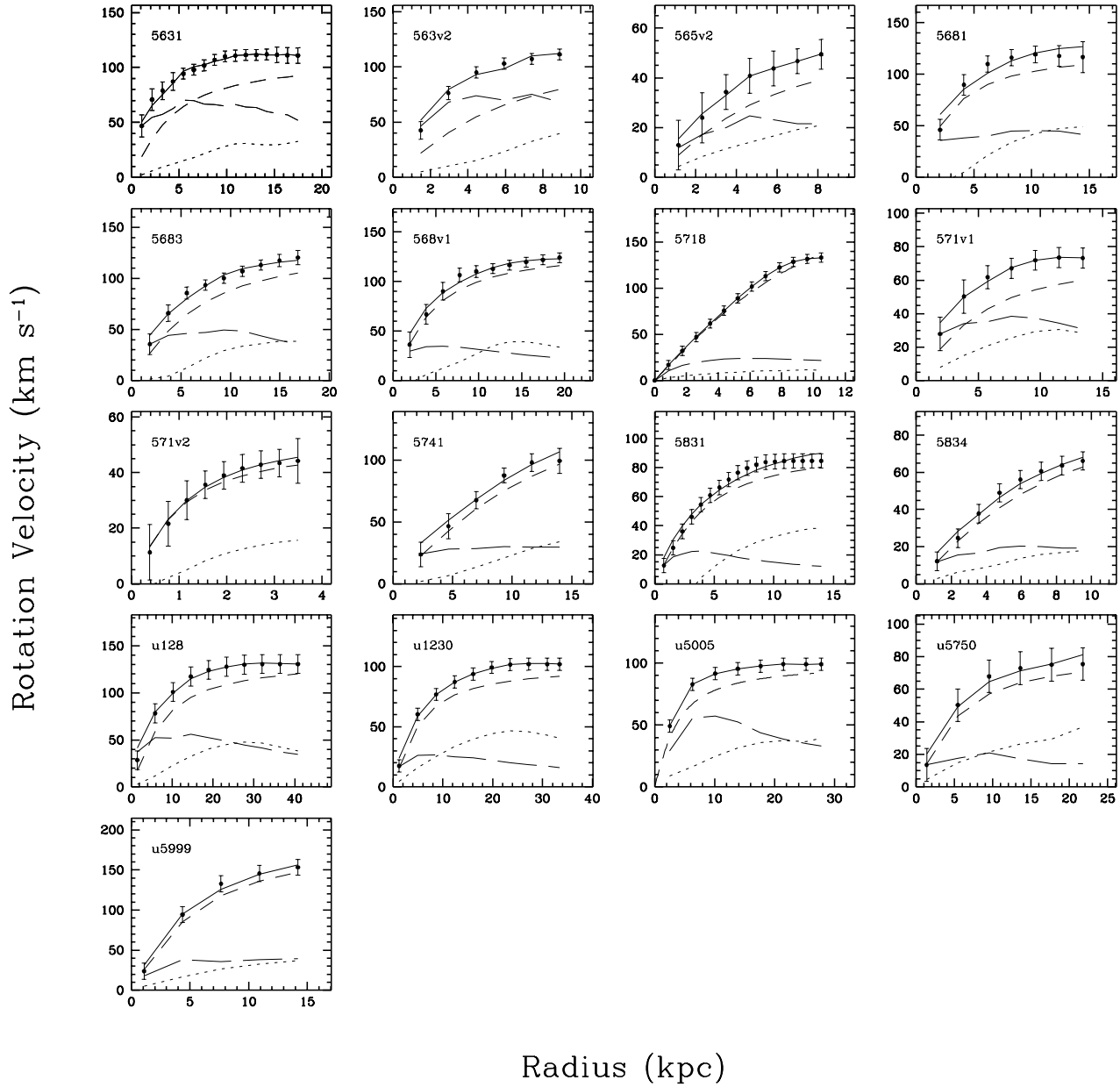
Figure 5. Maximum disk rotation curve decompositions of the final sample of LSB galaxies. The dotted lines represent the rotation curves of the gas; the long dashed line those of the scaled stellar disk; the short dashed lines the rotation curves of the halo. The full line represents the total model rotation curve. Error bars are based on a combination of profile width in the position-velocity diagrams (BMH96) and the asymmetries between the rotation curves of both sides of the galaxies. Shown are the R band decompositions, except for F563-V2 where we show the B band data due to lack of R data, and except for F571-V2 where the minimum disk solution is shown, as no optical photometry is available for that galaxy.

Table 4. Maximum disk decompositions of HSB sample (Broeils 1992)

Name	$\left(\frac{M}{L_B}\right)_\star$	R_C	V_∞	ρ_0	$M_{\rm d}$	$M_\star$	$M_{\rm gas}$
DDO154	1.2	2	59	15.3	0.39	0.01	0.04
DDO168	1.1	2.7	98	24.2	0.21	0.02	0.03
DDO170	2.7	2.3	75	19.2	0.85	0.03	0.06
N55	0.7	7.9	146	6.4	1.5	0.29	0.13
N247	4	7.3	136	6.54	1.33	0.95	0.1
N300	2	6.32	132	8.3	1.74	0.42	0.16
N801	4	74.3	302	0.3	19.14	23.83	2.86
N1003	1.1	9.7	133	3.5	7.83	0.82	0.82
N1560	3.5	6.8	133	7.2	0.94	0.12	0.1
N2403	1.8	6.6	154	10.2	6.26	1.39	0.43
N2841	5.1	21.7	308	3.7	116.1	23.97	2.09
N2903	2.9	3.2	166	51	12.52	4.48	0.34
N2998	2.1	24.8	242	1.8	26.95	13.79	3
N3109	0.5	8.7	141	4.9	0.76	0.04	0.06
N3198	3.5	7.6	156	7.8	11.25	3.11	0.69
N5033	5.3	5.9	170	15.2	18.23	9.84	0.91
N5533	6.8	34.6	255	1	52.89	30.05	3.2
N5585	0.5	1.8	99	56.9	1.63	0.06	0.17
N6503	1.7	2.5	115	38.6	5.74	0.83	0.22
N6674	4	119.5	655	0.6	53.36	20.92	3.9
N7331	5.8	103	982	1.7	32.42	12.95	1.58
U2259	3.4	6.1	137	9.5	0.94	0.35	0.05
U2885	2.1	44.9	382	1.3	1.87	37.37	4.8

Note: $(M/L_B)_\star$ is in units of $(M_\odot/L_{\odot,B})$; R_C is in units of kpc, V_∞ in units of km s^{-1}, ρ_0 is in units of 10^{-3} $M_\odot{\rm pc}^{-3}$; all masses are in units of $10^{10}M_\odot$. See Broeils (1992) and references therein.
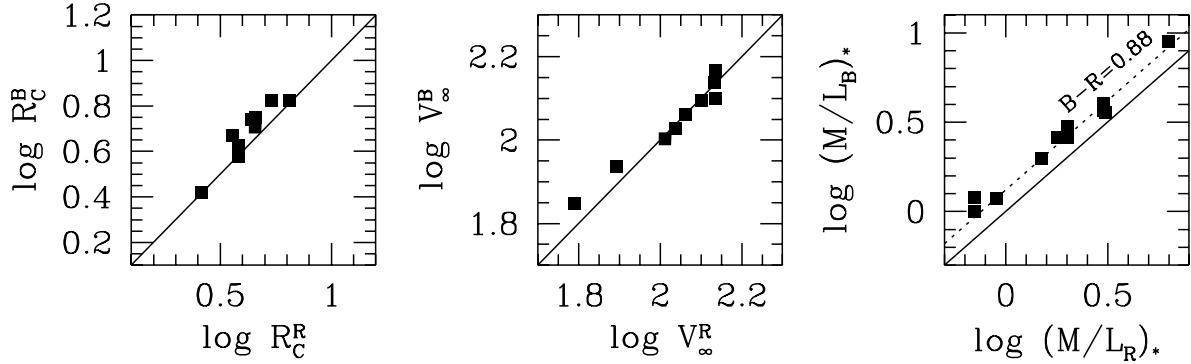

Figure 6. Comparison of the core radii R_C (left panel) and asymptotic velocities (middle panel) V_∞ of the halos, and the maximum disk mass-to-light ratio $(M/L)_\star$ of the stellar disk (right panel) resulting from separate B and R band decomposition of the rotation curves of the subset of LSB galaxies for which both R and B band photometry were available. The B and R band decompositions are consistent with each other. The full drawn lines are lines of equality. The dotted line in the right panel is the relation between $(M/L_B)_\star$ and $(M/L_R)_\star$ for $B - R = 0.88$.

Table 5. Bottema disk and minimum disk decompositions HSB sample

Name	Bottema disk[a]						Minimum disk[b]			
	$\left(\frac{M}{L_B}\right)_\star$	R_C	V_∞	ρ_0	M_d	$M_\star$	R_C	V_∞	ρ_0	M_d
DDO154	1.1	2.0	58.3	16.3	0.39	0.01	1.7	56.3	21.1	0.39
DDO168	1.0	2.0	79.3	29.7	0.23	0.002	1.5	77.8	51.2	0.23
DDO170	*	*	*	*	*	*	1.6	70.6	35.4	0.84
N55	1.3[d]	6.4	140.4	9.0	1.53	0.26	2.4	104.2	36.2	1.76
N247	1.4	3.7	93.9	12.1	1.38	0.90	1.4	107.3	114	2.11
N300	1.6	6.9	134.2	7.1	1.70	0.46	1.4	104.7	109	2.19
N801	1.8	9.3	178.2	6.8	29.35	13.62	–	–	–	–
N1003	1.3	4.3	104.2	11.0	8.06	0.59	–	–	–	–
N1560	1.4	2.4	87.4	24.1	1.01	0.05	1.8	84.1	40.6	0.96
N2403	1.3	2.7	131.6	44.3	6.73	0.92	0.8	134.3	470	7.95
N2841	2.0	4.0	266.3	80.4	130.4	9.63	–	–	–	–
N2903	1.7	0.4	175.2	3933	15.03	1.97	–	–	–	–
N2998	1.5	1.5	177.6	262.8	34.16	6.58	–	–	–	–
N3109	1.5[d]	8.7	141.0	4.9	0.76	0.04	3.5	92.5	12.6	0.81
N3198	1.4	1.4	138.7	189.6	12.88	1.48	–	–	–	–
N5033	1.5	0.04	181.0	378800	24.28	3.79	–	–	–	–
N5533	2.0	0.2	190.9	13930	69.18	13.76	–	–	–	–
N5585	1.4[d]	1.8	99.0	56.0	1.63	0.06	1.3	98.6	104	1.73
N6503	1.6	0.6	110.8	610.4	6.24	0.34	–	–	–	–
N6674	–[c]	23.6	247.1	2.0	59.93	14.34	–	–	–	–
N7331	–[c]	9.3	233.4	11.8	38.55	6.82	–	–	–	–
U2259	–[c]	1.2	81.2	89.1	1.07	0.22	0.4	88.5	948	1.27
U2885	–[c]	14.9	281.2	6.61	15.33	23.91	1.0	287.9	1656	136.2

Note: $(M/L_B)_\star$ is in units of $(M_\odot/L_{\odot,B})$ in the respective bands; R_C is in units of kpc, V_∞ in units of km s^{-1}, ρ_0 is in units of 10^{-3} $M_\odot$pc^{-3}; all masses are in units of $10^{10} M_\odot$.

a: The Bottema disk decompositions were taken from Rhee (1996).
b: A dash indicates that a minimum disk fit was not possible.
c: $(M/L_B)_\star$ not determined because of unknown contribution of bulge.
d: $(M/L_B)_\star$ is larger than maximum disk $(M/L_B)_\star$.

inal prescription cannot hold in LSB galaxies: 63% of the total rotation velocity is in many cases already more than the maximum disk solutions allow. In Appendix A we give a more general expression for $(M/L_B)_\star$ of a galactic exponential disk derived by Bottema (1997). The resulting $(M/L_B)_\star$ only depends on color, as the effects of luminosity and surface brightness cancel in this model. In the absence of data on stellar velocity dispersions of low or intermediate surface brightness galaxies, this is the best we can currently do taking into account the actual gravitational potential of the disk. In the following we will refer to this prescription as the "generalized Bottema-disk." Of course, when applying this generalized scheme to HSB galaxies, the original 63% criterion is retrieved.

The $(M/L)_\star$ values given in column (20) of Table 3 show that the range of values implied by the Bottema disk is very small compared to the maximum disk values. This is due to the relatively small range in $B-V$ colors shown by the galaxies. We have used Bottema's original "63% recipe" (as presented in Rhee 1996) for galaxies with $\mu_0^B < 23$ mag arcsec^{-2}, while the generalized Bottema disk was used for galaxies with μ_0^B fainter than this value, where 63% of the total rotation velocity is already more than maximum disk allows. In practice the generalized disk was thus

used for the LSB galaxies, NGC 247 and the three DDO galaxies. For NGC 55, NGC 3109 and NGC 5585 the Bottema recipes resulted in $(M/L_B)_\star$ values larger than those implied by maximum disk and we have assumed the maximum disk values. In at least one case (NGC 3109) it can be shown that the discrepancy arises because of a large difference between the optical (Fabry-Perot) and HI rotation curves. If the Fabry-Perot curve is used the maximum disk $(M/L_B)_\star$ value becomes larger than the Bottema value.

5 RESULTS OF DECOMPOSITIONS

5.1 The influence of resolution on disk-halo decompositions

As we have established in Section 3 that beam-smearing is not determining the shapes of the rotation curves, we should not expect the results of disk-halo decompositions of the LSB galaxies to be influenced significantly by resolution effects. We test this by again looking at the case of NGC 1560 (Figure 4).

Even the high-resolution decompositions of this galaxy are not entirely unambiguous, showing that even in a maximum disk decomposition it is difficult to entirely constrain
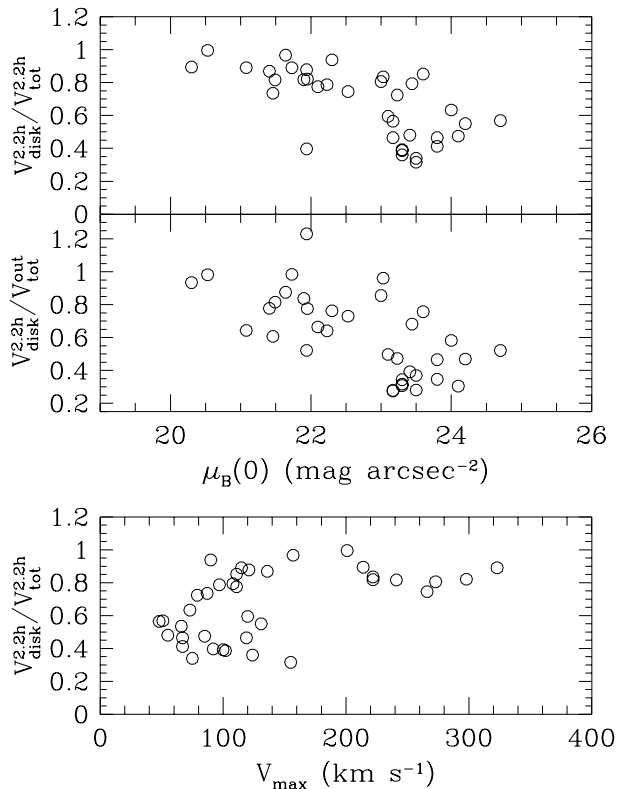
Figure 7. Top panel: the ratio of the peak rotation velocity of the maximum disk and the observed total rotation velocity at $2.2h$. This ratio is approximately constant at ~ 0.85 for galaxies with $\mu_0(B) < 23$ mag arcsec^{-2} and drops steeply to values of ~ 0.5 for the LSB galaxies. Even at $2.2h$ the importance of the disk decreases toward lower surface brightnesses, despite higher values of $(M/L)_\star$. Middle panel: the ratio of the peak rotation velocity of the maximum disk and the observed total rotation velocity at the outermost measured point. This ratio also changes systematically with surface brightness, from ~ 1 for the highest surface brightness galaxies, where the disk determines the maximum rotation velocity, to ~ 0.3 for LSB galaxies, where the halo completely determines the dynamics of these galaxies. Bottom panel: the ratio of maximum disk peak velocity and observed velocity at $2.2h$. At $V_{\max} < 150$ km s^{-1} a range of ratios is observed, from ~ 0.85 for HSB galaxies to ~ 0.4 for LSB galaxies. The lack of points with low ratios at $V_{\max} > 150$ km s^{-1} might be caused by selection effects: LSB galaxies with such large rotation velocities have not yet been mapped in H I.

Table 6. Halo parameters of NGC 1560

	high res.	low res.
$(M/L_B)_\star$	3.5	4
V_∞	133	121
R_C	6.8	6.2
ρ_0	7.2	5.9

the $(M/L)_\star$ value. The quoted maximum disk $(M/L_B)_\star$ values range from 3.5 (Broeils 1992, Chapter 10) and 4.1 (Begeman, Broeils & Sanders 1991) to 4.9 (Broeils 1992, Chapter 5). The latter case is however an attempt to fit the data without a dark halo, and we will discard that value. To be consistent with Tables 1 and 4 we adopt $(M/L_B)_\star = 3.5$. This maximum disk decomposition is shown in the left panel of Fig. 4. Corresponding halo parameters, taken from Table 3 are repeated in Table 6.

As described in Sect. 3.3, the rotation curves of NGC 1560 were smoothed from a resolution of 38 beams to 3 beams. We have attempted a maximum disk decomposition on this low resolution data, and find that, although again there is some freedom in $(M/L)_\star$, the best-fitting value for the low-resolution data is $\simeq 4$. We can exclude $(M/L_B)_\star = 3$ or 5 as possible solutions for this particular case, as the corresponding low-resolution models systematically over- or under-estimate the rotation velocities at certain radii. The low-resolution halo parameters are given Table 6, and are comparable with the high-resolution values.

The value $(M/L_B)_\star = 4$ for the low-resolution case was determined by simply scaling the stellar rotation curve to match the innermost point. This procedure is thus for the low resolution case equivalent to a formal maximum disk fit in the high-resolution case. Studying high-resolution curves in detail shows that this scaling to match the innermost point is usually what happens in practice when doing a formal maximum disk fit.

5.2 Maximum disk mass-to-light ratios

As is clear from Fig. 5, the rotation curves of the stellar disks in the LSB galaxies (even in the maximum disk case) do not even approach the maximum rotation velocities of the observed rotation curves. This is in sharp contrast with HSB galaxies where the rotation curve of the stellar disk is usually able to explain most of the rotation velocity in the inner parts.

This is also illustrated in the top panel of Fig. 7. This shows the ratio of the peak velocity of the maximum disk at $2.2h$ and the total observed rotation velocity at that radius. At central surface brightnesses brighter than 23 B-mag arcsec^{-2}, the maximum disk can account for $85\% \pm 10\%$ of the total rotation velocity, but this rapidly drops to only 40% or less for LSB galaxies.

This increasing inability of the maximum disk to explain the observed rotation velocities is illustrated in the middle panel of Fig. 7, which shows the ratio of the peak velocity of the maximum stellar disk and the maximum observed rotation velocity. This ratio systematically changes from ~ 0.9 at high surface brightnesses (i.e. the disk defines

the maximum rotation velocity and the halo "conspires" to keep the rotation curve flat) to values of ~ 0.3 for the LSB galaxies (i.e. the halo completely determines the dynamics of the galaxies). The bottom panel of Fig. 7 again shows the ratio of of the peak velocity of the maximum disk at $2.2h$ and the total observed rotation velocity at that radius, but as a function of $V_{\max}$.

The maximum disk $(M/L)_\star$ values are shown in Fig. 8 as a function of μ_0^B, $V_{\max}$ and $B-V$. The relation between $(M/L_B)_\star$ and $V_{\max}$ (top-left) shows a clear segregation between galaxies of different surface brightnesses: at each value of $V_{\max}$ the HSB galaxies have the lowest value of $(M/L_B)_\star$ while the LSB galaxies always show high $(M/L_B)_\star$ values. Also shown is the relation $(M/L_B)_\star \propto L^{1/2}$ which was previously derived for HSB galaxies by e.g. Ashman, Salucci & Persic (1993) and Broeils (1992). Clearly the conclusion that late-type (i.e. lower surface brightness) galaxies have smaller maximum disk stellar mass-to-light ratios than early-type (i.e. higher surface brightness) galaxies was, in the light of this new data, a selection effect. The maximum disk $(M/L_B)_\star$ is not a simple function of L (or $V_{\max}$) alone, but also depends on surface brightness.

The absence of a relation between $(M/L_B)_\star$ and μ_0 (top-center) is a result of comparing galaxies with different global properties: at each $V_{\max}$ there is a large range in μ_0 (and consequently a large range in $(M/L_B)_\star$). Comparing galaxies at fixed μ_0 means comparing galaxies of different masses and luminosities.

The surface brightness segregation effect at fixed $V_{\max}$ cannot be an artificial effect caused by the lower resolution of the LSB observations. We have shown in Section 3 that beam smearing effects are potentially most severe in HSB galaxies. If beam-smearing were to have affected the LSB curves this would imply even higher values for $(M/L)_\star$, thus making the difference between HSB and LSB galaxies seen in Fig. 8 even more dramatic (see also discussion in de Blok & McGaugh 1996).

5.2.1   The maximum exponential disk

The segregation in $(M/L)_\star$ can be explained from the properties of the exponential disk and the systematics of maximum disk fitting. As LSB galaxies obey the same Tully-Fisher relation as HSB galaxies (Zwaan et al. 1995), this requires LSB galaxies to have larger scale lengths at fixed $V_{\max}$, in order to still reach the required value of L. The maximum rotation velocity of an exponential disk is given by $v \propto \sqrt{\sigma_0 h}$, where σ_0 is the central mass surface density. In practice the value of σ_0 is not known, and the distribution of the light is used to compute the rotation curve of the disk. This rotation curve of the light has a maximum rotation velocity of

$$v_1 \propto \sqrt{\Sigma_0 h}, \tag{5}$$

where Σ_0 is the central surface brightness in linear units. (In the following we will denote the rotation velocity of the disk with v, while the observed total rotation velocity will be indicated with V.) In the rotation curve fitting process the mass-to-light ratio $(M/L)_\star$ is introduced to convert surface brightness to mass surface density and compute the disk rotation curve. Under the maximum disk hypothesis $(M/L)_\star$

is scaled to its maximum possible value. The peak rotation velocity of the maximum disk is then given by

$$v_{\rm m} \propto \sqrt{(M/L)_\star \Sigma_0 h}. \tag{6}$$

From Eqs. (5) and (6) it is clear that

$$\left(\frac{M}{L}\right)_\star = \left(\frac{v_{\rm m}}{v_1}\right)^2. \tag{7}$$

We will now compare a HSB and a LSB galaxy at identical positions on the Tully-Fisher relation. We find for the peak velocity of the rotation curve of the light in the HSB, $v_1^{\rm H}$, that $(v_1^{\rm H})^2 \propto (\Sigma_0^{\rm H} h^{\rm H})$, and for the peak velocity in the LSB, $v_1^{\rm L}$, that $(v_1^{\rm L})^2 \propto (\Sigma_0^{\rm L} h^{\rm L})$, where $\Sigma_0^{\rm L,H}$ and $h^{\rm L,H}$ are the central surface brightnesses and scale lengths of the LSB and the HSB, respectively. As their luminosities $L \propto \Sigma_0 h^2$ are identical we find $h \propto \Sigma_0^{-\frac{1}{2}}$ and we can write $v_1^{\rm L}$ as

$$(v_1^{\rm L})^2 \propto \Sigma_0^{\rm L} h^{\rm L} \propto \frac{\Sigma_0^{\rm L}}{\Sigma_0^{\rm H}} \Sigma_0^{\rm H} \left(\frac{\Sigma_0^{\rm H}}{\Sigma_0^{\rm L}}\right)^{\frac{1}{2}} h^{\rm H} \propto \left(\frac{\Sigma_0^{\rm L}}{\Sigma_0^{\rm H}}\right)^{\frac{1}{2}} (v_1^{\rm H})^2. \tag{8}$$

Using Eqs. (7) and (8) we express $(M/L)_\star^{\rm L}$ in term of $(M/L)_\star^{\rm H}$.

$$
\begin{aligned}
\left(\frac{M}{L}\right)_\star^{\rm L} &= \left(\frac{v_{\rm m}^{\rm L}}{v_1^{\rm L}}\right)^2 = \left(\frac{\Sigma_0^{\rm H}}{\Sigma_0^{\rm L}}\right)^{\frac{1}{2}} \left(\frac{v_{\rm m}^{\rm L}}{v_1^{\rm H}}\right)^2 \\
&= \left(\frac{\Sigma_0^{\rm H}}{\Sigma_0^{\rm L}}\right)^{\frac{1}{2}} \left(\frac{v_{\rm m}^{\rm H}}{v_1^{\rm H}}\right)^2 \left(\frac{v_{\rm m}^{\rm L}}{v_{\rm m}^{\rm H}}\right)^2 \\
&= \left(\frac{\Sigma_0^{\rm H}}{\Sigma_0^{\rm L}}\right)^{\frac{1}{2}} \left(\frac{v_{\rm m}^{\rm L}}{v_{\rm m}^{\rm H}}\right)^2 \left(\frac{M}{L}\right)_\star^{\rm H}.
\end{aligned} \tag{9}
$$

For galaxies at identical positions on the Tully-Fisher relation, the ratio of their maximum disk $(M/L)_\star$ values thus depends on the ratio of the surface brightnesses and the ratio of their peak rotation velocities. This latter ratio depends on the shape of the rotation curves or, more specifically, the change of shape with surface brightness at fixed $V_{\max}$. We have already seen that the rotation curves of LSB galaxies rise more slowly than those of HSB galaxies, so we expect the peak velocities of the maximum disk of the LSB galaxies to be smaller than those of the HSB galaxies.

In order to get $(M/L)_\star^{\rm L} > (M/L)_\star^{\rm H}$, Eq. (9) requires that

$$\left(\frac{v_{\rm m}^{\rm L}}{v_{\rm m}^{\rm H}}\right)^4 \geq \frac{\Sigma_0^{\rm L}}{\Sigma_0^{\rm H}}. \tag{10}$$

It is easy to show that if both LSB and HSB galaxies had flat rotation curves, we find that $(M/L)_\star^{\rm L} > (M/L)_\star^{\rm H}$ always. In practice, at each $V_{\max}$ a large range of $v(2.2h)/V(2.2h)$ is found (Fig. 7). For the current sample, where a typical HSB galaxy has $\mu_0 \simeq 21.5$, while a typical LSB galaxy has $\mu_0 \simeq 24$, we find that condition (10) requires $v_{\rm m}^{\rm L}/v_{\rm m}^{\rm H} 0.5$ on average. We find the largest range of $v(2.2h)/V(2.2h)$ at $V_{\max} \simeq 100$ km s^{-1} in the bottom panel of Fig. 7. Taking the ratio of the average value for the LSB galaxies $v(2.2h)/V(2.2h) \simeq 0.45$ and that of the HSB galaxies $v(2.2h)/V(2.2h) \simeq 0.85$, yields a value of $v_{\rm m}^{\rm L}/v_{\rm m}^{\rm H} \simeq 0.5$. So although there will be individual cases where condition (10) will not hold (as is shown by the overlap of HSB and LSB points in the top-left panel of Fig. 8), *on average* condition (10) is always fulfilled, and we find that the intrinsic properties of the exponential disk
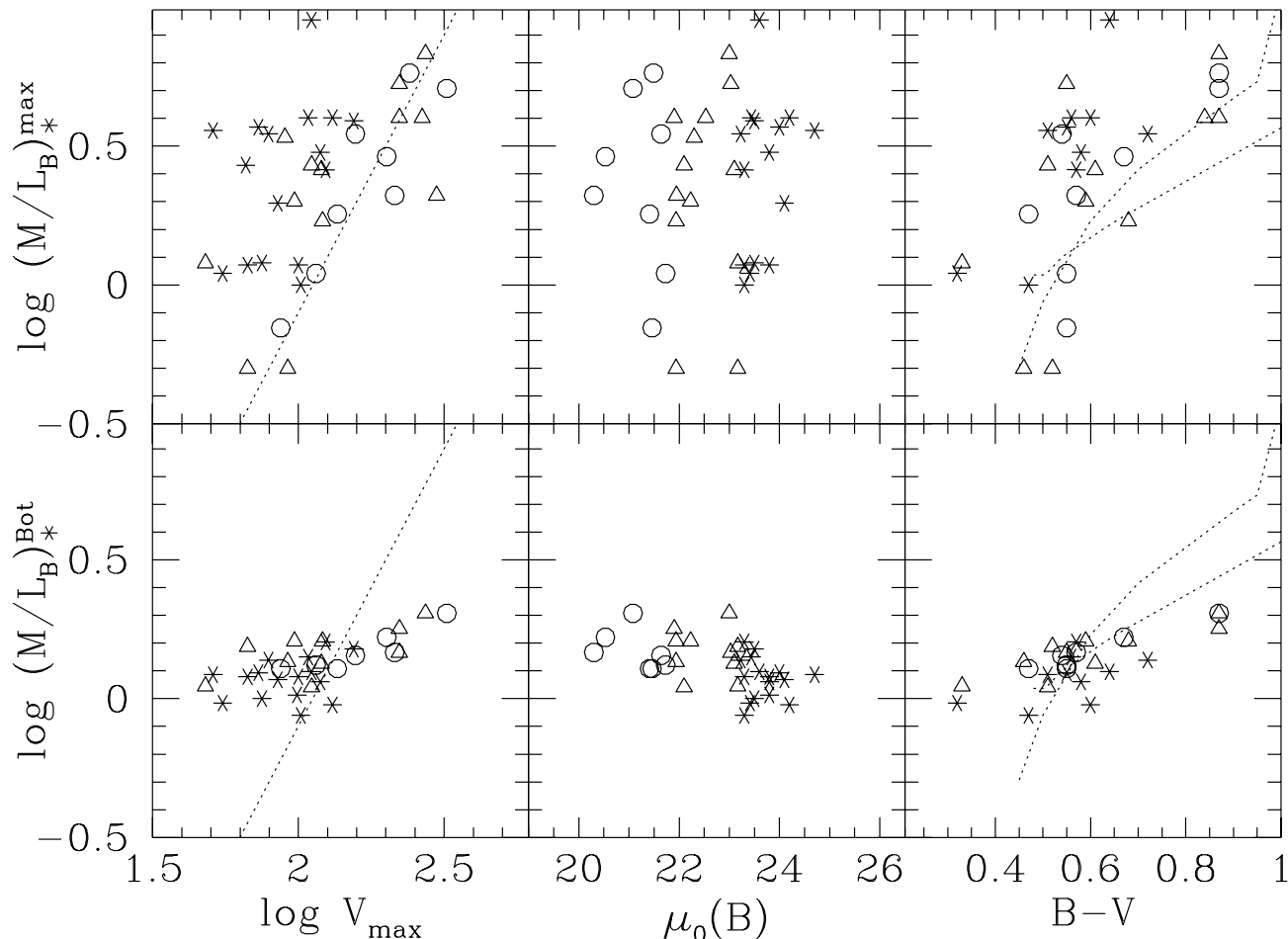
Figure 8. Top row: The maximum disk B-band stellar mass-to-light ratio plotted versus maximum rotation velocity (left panel), central surface brightness (middle panel), and average $B - V$ color (right panel). The open circles denote galaxies with $\mu_0(B) < 21.9$ mag arcsec^{-2}, the triangles represent $21.9 \leq \mu_0(B) < 23.2$ mag arcsec^{-2} galaxies and the asterisks galaxies with $\mu_0(B) \geq 23.2$ mag arcsec^{-2}. In the left panel the dotted line shows the relation $(M/L_B)_\star \propto L^{1/2}$. The relation has been arbitrarily shifted to follow the filled HSB data points. In the right panel the steep upper dotted curve shows the colour–mass-to-light ratio track from Larson & Tinsley (1978) while the shallow lower dotted curve shows the track as derived by Jablonka & Arimoto (1992). Both curves have been shifted to go through $\log(M/L_B)_\star = 0.55$ at $B - V = 0.55$ (see bottom-right panel). **Bottom row:** Idem, but now showing the B-band stellar mass-to-light ratio as derived assuming a Bottema disk.

combined with the maximum disk recipe always yield larger values of $(M/L)_\star$ for LSB galaxies than for HSB galaxies. No assumptions have been made on the stellar populations, ages, or evolution of the galaxies. The larger *fitted* maximum disk stellar mass-to-light ratios for LSB galaxies at fixed V_{max}, therefore do not need to reflect the true evolutionary stellar mass-to-light ratio of the disk.

5.2.2 Population effects?

But is it in fact at all possible to explain the systematically higher maximum disk $(M/L)_\star$ ratios of the LSB galaxies at fixed V_{max} in a consistent way by invoking systematic changes in the stellar populations? The systematically larger ratios imply an increasingly more evolved population with decreasing surface brightness: population synthesis models (Larson & Tinsley 1978) show that $(M/L_B)_\star$ of an evolv-

ing stellar population is in general an increasing function of time, and hence of increasing $B - V$ color.

Two examples are shown in in the right panels of Fig. 8, where the upper dotted line represents $(M/L_B)_\star$ as a function of the $B - V$ color of a stellar population with a declining star formation rate (Larson & Tinsley 1978). The lower dotted line is the track as derived by Jablonka & Arimoto (1992) who have used a model which also takes into account chemical enrichment.

To a certain degree the maximum disk results agree with the trend of increasing $(M/L_B)_\star$ with redder $B - V$: the lower envelope of the distribution of the points increases with redder color. Uncertainties in the low-mass end of the IMF make it very hard to derive absolute $(M/L_B)_\star$ values from any population synthesis model. This uncertainty may therefore shift the model track up or down, while e.g. metallicity effects may make the slope of the track more shallow (as the Jablonka & Arimoto track shows). However, the ob-

served range at each color is too large to be explained by models with a constant IMF and where the star formation history is well-behaved and a smoothly varying function of Hubble type.

The high maximum disk $(M/L)_\star$ are furthermore in direct conflict with observational evidence on colors (McGaugh & Bothun 1994, de Blok et al. 1995), metallicities (McGaugh 1994) and gas-fractions (McGaugh & de Blok 1997). As the stellar populations of LSB galaxies are in an earlier evolutionary state than HSB galaxies (van den Hoek et al. 1997) one would expect them to have *lower* values of $(M/L)_\star$. The values of $(M/L_B)_\star$ as derived under the maximum disk hypothesis are therefore *not* representative for the stellar population in LSB galaxies.

5.2.3 Disk dark matter?

Trying to explain the maximum disk results in a physical way, while having a stellar population with a lower $(M/L)_\star$ than implied by the maximum disk values, requires an additional dark component in the disk which traces the stellar population. This component has to become increasingly important towards lower central surface brightnesses. This might be an invisible baryonic component like e.g. cold molecular gas. There has already been much speculation about this in the literature (e.g. Pfenniger, Combes & Martinet 1994). LSB galaxies would be the ideal test cases for such theories as the major part of their disks should then be made up of this baryonic DM. Again, this component should be of increasing importance towards lower surface brightnesses.

This creates the unattractive picture of two dominant but distinct and differently distributed dark components: one that has to provide the extra mass in the disk to make it satisfy the maximum disk boundary condition, and one that has to provide the surplus velocity in the outer parts to produce the observed rotation curves. These two dominant components then have to "conspire" to produce the observed rotation curve. Either way, DM remains of extreme importance in LSB galaxies.

5.2.4 Non-maximum disk

Another possibility is that disks are simply non-maximal. Part of the halo DM is wrongly attributed to the disk simply because the disk does not dominate the dynamics in the inner parts. This could in principle affect the derived values for the structural parameters of the halo, but this is only of minor importance in LSB galaxies. They are DM dominated, irrespective of the value of $(M/L)_\star$, so that changing the mass of the disk does not really matter. It is, however, of crucial importance in HSB galaxies where the disk is dominant, and the halo parameters therefore sensitive to the precise value of $(M/L)_\star$.

The maximum disk hypothesis, in combination with the extendedness of LSB galaxies thus produces a balancing act where LSB galaxies have to have large $(M/L)_\star$ ratios, or extra dark components, which are contrary to what we can derive from other evidence (stellar populations, metallicity, gas fraction). Maximum disk is therefore not the preferred way of making mass models in LSB galaxies.

5.3 Maximum disk halo parameters

For the LSB galaxies the asymptotic velocity V_∞ is well correlated with the observed maximum rotation velocity V_{max}, showing that although many of the LSB curves are still rising in the outermost point, they are close to their true maximum velocity. We will use this observational parameter instead of the fitted V_∞. Figure 9 summarizes the halo parameters for the HSB and LSB galaxies under the assumption of maximum disk. The core radius R_C is rather constant, both as a function of V_{max} and μ_0. The group of points at large R_C belong to HSB galaxies that are very much dominated by luminous matter, and are maximum disk in the true sense of the word: their inner rotation curve can be explained completely by that of the disk. To avoid having a hollow halo in these galaxies, the maximum disk $(M/L)_\star$ is usually slightly, but somewhat arbitrarily, lowered. The halo parameters are extremely sensitive to this. In most cases these galaxies have a bulge, that also has to be accommodated in the fitting procedure, with its own uncertainties in its $(M/L)_\star$. The HSB points at large R_C are thus uncertain.

The central halo densities ρ_0 as a function of μ_0 tend to be somewhat higher than those of HSB galaxies, but again, the uncertainty in the decompositions of the HSB galaxies makes it difficult to say anything more definite.

The ratio between core radius and optical scale length changes with surface brightness from $R_C \simeq 3h$ for the HSB galaxies to $R_C \simeq h$ for the LSB galaxies. In the maximum disk picture the optical disks of LSB galaxies are massive and extend further out into the halo.

5.4 Minimum disk

We can illustrate that the halo parameters derived for the LSB galaxies are robust values, by comparing the values derived for maximum disk and minimum disk. This is done in Fig. 10, where the core radii and central densities as derived using these two extreme hypotheses are compared. The difference in maximum and minimum disk halo parameters is clearly a strong function of surface brightness. The largest difference is observed for the HSB galaxies, where the central density ρ_0 changes by more than an order of magnitude. A similar conclusions applies to the core radius. This is in sharp contrast with the core radii derived for the LSB galaxies. The minimum disk values differ from the maximum disk values by less than a factor of two. The slope of the trend with surface brightness changes from negative to positive when going from maximum disk to minimum disk. This is entirely caused by the large change in parameters of the HSB galaxies.

The DM dominance makes the parameters of the LSB galaxy halos insensitive to the precise $(M/L)_\star$ value. The values we derive for the halo structural parameters, but also for the dark mass in these halos, are therefore likely to be very close to their true values.

5.5 Bottema disk mass-to-light ratios

The most important property which distinguishes the Bottema disk from the maximum disk is its small range of $(M/L_B)_\star$. This is immediately apparent in Fig. 8. The Bottema disk typically implies values of $(M/L_B)_\star$ between 1
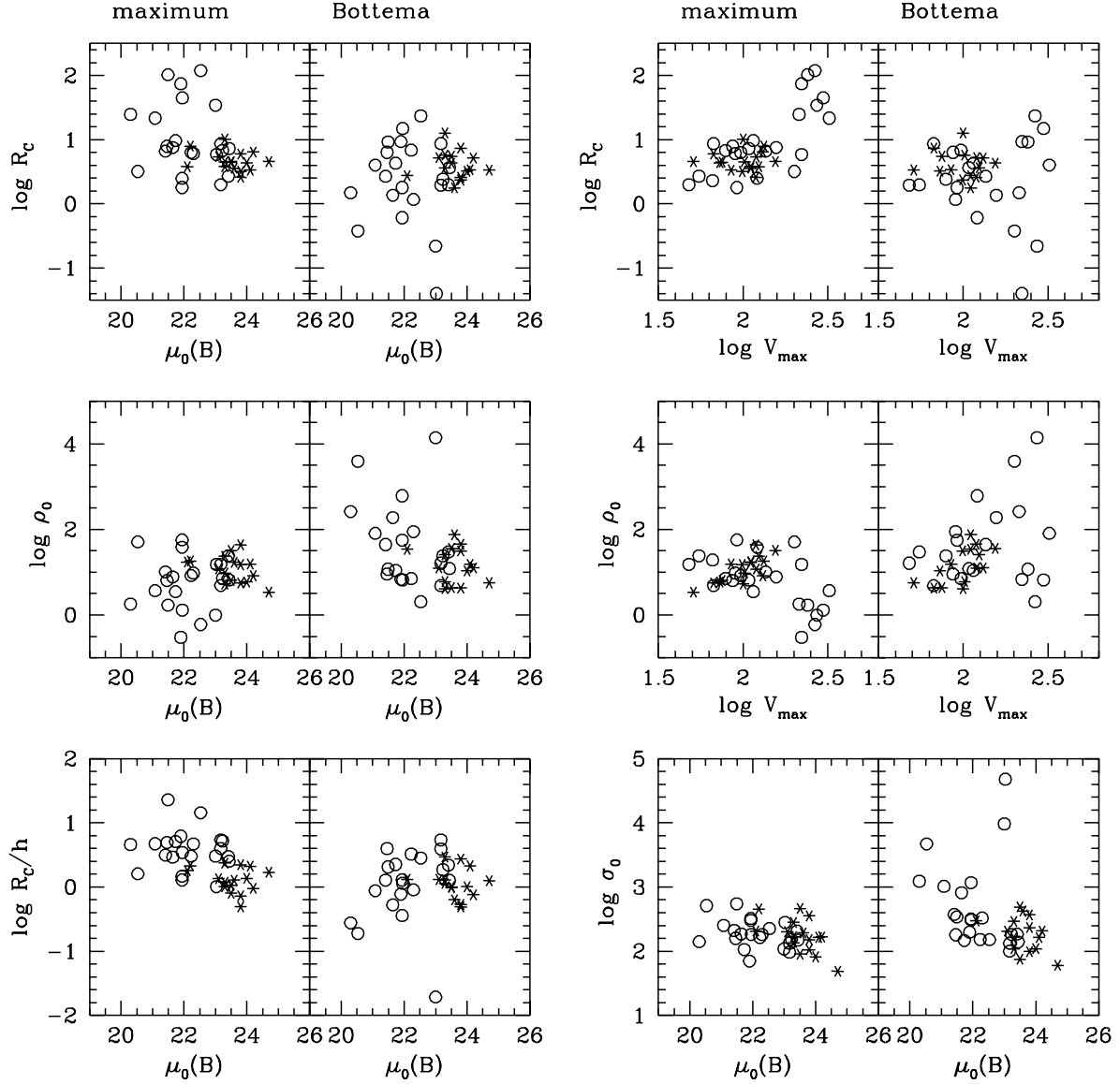
Figure 9. Isothermal halo fitting parameters for maximum disk fits (left panels) and Bottema disk fits (right panels). The open circles represent the HSB sample, the asterisks the LSB sample. ρ_0 is expressed in units of $10^{-3} M_\odot \ pc^{-3}$; R_C in kpc; σ_0 in $10^{-3} \ M_\odot \ pc^{-2}$; V_{max} in km s^{-1}; and $\mu_0(B)$ in mag arcsec^{-2}.
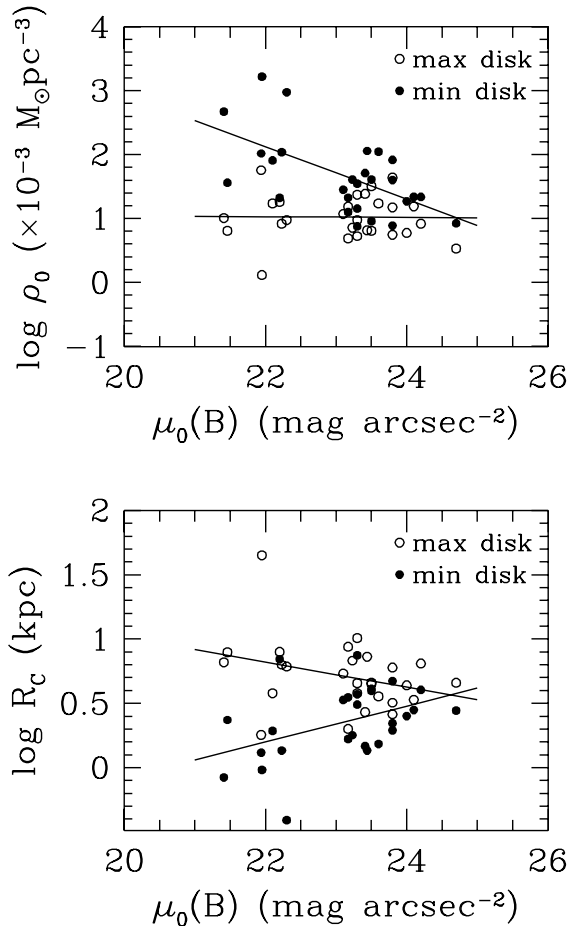
Figure 10. The central densities (top) and core radii (bottom) of the halos HSB and LSB galaxies under the maximum disk assumption (open circles) and minimum disk assumption (filled circles). The core radii and densities of the HSB galaxies are more affected by the respective assumptions than those of the LSB galaxies. Note the different slopes of the trends under the different hypotheses. The drawn lines are least-squares fits.

and 2. In general the reddest galaxies have the highest mass-to-light ratios.

The striking systematic offset in $(M/L)_\star$ at fixed V_{max} between HSB and LSB galaxies for the maximum disk hypothesis has disappeared (compare with top left panel in Fig. 8). At fixed V_{max} galaxies now have approximately identical $(M/L)_\star$ ratios. The majority of the data points has a much smaller spread and is in much closer agreement with stellar population models (Larson & Tinsley 1978; van den Hoek et al. 1997) than the maximum disk values. The need for an extra dark component in the disk has disappeared.

5.6 Bottema disk halo parameters

Whereas in the maximum disk case the galaxies with the highest values of V_{max} have the lowest central halo densities, in the Bottema disk case they have the densest and most

compact halos. The central densities of the galaxies with low V_{max} are, as expected, less affected. The large change in halo parameters of HSB galaxies compared to their maximum disk values, results in trends of halo density and core radius opposite to those derived for maximum disk.

Paradoxically, the uncertainties in the decompositions of the *HSB* galaxies makes it very hard to make definite statements on the halo properties and their possible changes with surface brightness.

5.7 Halo parameters and galaxy evolution

Generalizing (and running the risk of over-interpreting) the maximum disk and Bottema disk decompositions leads to two distinct different sets of relations between the dark and visible components of galaxies. The maximum disk decompositions suggest that at fixed V_{max} all halos are equal, while the Bottema disk decompositions suggest that the sizes and densities of DM halos are directly related to those of the optical disks that inhabit these halos. In summary:

(i) **Maximum disk** Towards lower surface brightnesses halos become denser and smaller. Disks of lower surface brightness have higher $(M/L)_\star$ at fixed V_{max}, and extend further out into the halo.
(ii) **Bottema disk** Towards lower surface brightnesses halos become more diffuse and more extended. Disks of lower surface brightness have similar $(M/L)_\star$ at fixed V_{max} and are found in more massive halos.

Option (i) implies that the dimmest and most extended (LSB) galaxies live in the most compact halos. Presumably the collapse of their massive, dark disks was not as complete as in HSB galaxies (because of the larger angular momenta of LSB galaxies?).

With option (ii) the properties of the baryonic part of the galaxy are reflected in those of the host halo: dim, diffuse and extended galaxies inhabit extended, low density halos. In both cosmologies the dominance of DM increases towards lower surface brightnesses.

5.7.1 Maximum disk cosmology

If, for the moment, we assume the maximum disk results to hold, what are the implications for the evolution of LSB galaxies? In other words, what if the only difference between HSB and LSB galaxies at fixed V_{max} is that LSB galaxies stick out further into otherwise identical halos?

The picture which can then be sketched is deceivingly simple. For a HSB and a LSB galaxy at identical positions on the TF relation, the LSB galaxy has to be more extended optically (Zwaan et al. 1995), and in order to have the same luminosity as the HSB galaxy, the amount of past and present star formation per area (the surface brightness) has to be lower[†]. The LSB optical disk simply encompasses more DM than the HSB optical disk, due to its larger extent

---

[†] The bluer colors of LSB galaxies are explained by metallicity effects and the less prominent old population. An equal amount of star formation has a much larger effect on the colors of a LSB galaxy than on a HSB galaxy (de Blok et al. 1995).

in an otherwise identical halo, resulting in a LSB optically extended galaxy with a high total (i.e. DM and luminous matter) M/L. The low star formation rate (as averaged over the lifetime of the galaxy) implies slow evolution in the LSB galaxy and a low $(M/L)_\star$ [‡], which is difficult to reconcile with the maximum disk hypothesis assumed to hold to derive the these conclusions.

Current ideas on the formation and evolution of LSB galaxies (Bothun et al. 1993, McGaugh 1992, Mo et al 1994, Dalcanton et al. 1997) suggest that LSB galaxies form from lower amplitude density peaks than HSB galaxies. As they are also found to be more isolated from their neighbors, and to have a lack of companions with respect to HSB galaxies, they have presumably also undergone less interaction with other galaxies. The extended gas disks also suggest that the collapse of the baryonic matter has been much less efficient than in actively star forming HSB galaxies.

Although the Bottema disk solution may seems the most one, both solutions do have their problems. The maximum disk solution has to explain why galaxies in otherwise identical halos have different collapse-histories as a function of surface brightness, while the other solution has to explain how galaxies with different halo masses but identical luminosities conspire to still end up at the same position on Tully-Fisher relation.

One conclusion is firm however, the dynamics of LSB galaxies are fundamentally different from those of HSB galaxies. For example, the rotation curves of LSB galaxies can not be explained in $\Omega_0 = 1$ cosmological simulations (Moore 1994, Navarro 1997), which is a problem, certainly in view of the implied numerical richness of LSB galaxies (McGaugh 1995).

6 MASS RATIOS

6.1 Importance of atomic gas

The increasing dynamical importance of the gas component can readily be seen in Fig 11a and b. Galaxies of lower surface brightnesses have larger values of $M_{gas}/M_\star$. A similar trend with Hubble type was already noticed by e.g. Broeils (1992). The trend is clear in both the maximum disk and Bottema cases, although of course the gas-to-stellar mass ratios derived using maximum disk stellar masses tend to be larger. The ratio ranges from ~ 0.2 for the HSB galaxies, to ~ 2 in the LSB galaxies. Clearly in LSB galaxies the gas component can be of a larger dynamical importance than the stellar component, even in the maximum disk case. This effect is more pronounced for the Bottema decompositions because of the limited range in $(M/L)_\star$. A fuller discussion of the gas fraction over a large range in surface brightness is presented in McGaugh & de Blok (1997).

M_{gas}/M_{dark} (as computed within the outermost measured point of the rotation curve, R_{max} (see Table 1), and assuming Bottema disk) is shown in Fig. 11c and e. Panels d and f show M_{gas}/M_{dark} measured within $5h$. There is

clear trend of increasing gas-richness towards low values of V_{max}, an effect which is not entirely cancelled when measured within $5h$. Slower rotating galaxies contain relatively more gas. The large range in μ_0 found at each V_{max} ensures that no clear trend is visible of M_{gas}/M_{dark} with μ_0.

6.2 Baryon fraction and dark matter fraction

The total luminous mass M_{lum} is defined as the sum of stellar mass and the gas mass. We here take the stellar mass as implied by the Bottema disk. The ratio of the dark and luminous mass is related to the maximum velocity (or luminosity) (Persic & Salluci 1991, Broeils 1992). Galaxies with low maximum velocities and low luminosities are more DM dominated than high luminosity galaxies. This effect is not very pronounced when M_{dark} is computed within the outermost radius (Fig. 11g and i): the extended and well-observed rotation curves of HSB galaxies encompass a relatively much larger fraction of the halo. The effect becomes much more pronounced when measured within a fixed number of scale lengths (Fig. 11h and j).

The extreme DM domination of the lowest surface brightness galaxies has more general implications. One example is the baryon fraction f_b of the universe. This is of direct cosmological significance since $\Omega_0 = \Omega_b/f_b$, where Ω_b is the baryon density of the universe: a measure of f_b combined with Ω_b from primordial nucleosynthesis directly yields Ω_0.

A value of f_b thought to be representative of the universal baryon fraction is given by X-ray observations of galaxy clusters (White et al. 1993; David et al. 1995; White & Fabian 1995): $0.1 < f_b < 0.2$. A similar result is obtained for compact groups of galaxies (Pildis et al. 1995). Primordial nucleosynthesis gives $\Omega_b = 0.022$ (e.g. Walker et al. 1991); together these suggest $\Omega_0 \approx 0.2$.

Now consider the rotation curve data. Dark matter is required to keep the rotation curves flat, and since there is no indication of declining rotation curves, the halos must be substantially larger than the last measured point. The dark to luminous mass within R_{max} therefore gives an upper limit on f_b (Fig. 11), through $f_b < (M_{lum}/M_{tot})$ and therefore

$$f_b < \left(1 + \frac{M_{dark}}{M_{lum}}\right)^{-1}.$$

To be conservative, let us consider the maximum disk case. For most HSB galaxies, R_{max} is not sufficiently large to provide an interesting limit. However, the DM domination of LSB galaxies improves this situation. In our sample, there are a few galaxies for which the upper limit on f_b is lower than the lower bound of the range of the cluster baryon fractions. These are F568–V1, UGC 5750, UGC 5999 (all with $f_b < 0.08$), and F571–8 ($f_b < 0.05$) (although this latter value is uncertain due to the inclination of the galaxy). The rotation curves of all four of these galaxies are flat or rising at the last measured point, so the dark halos must extend well beyond R_{max} to avoid having a perceptible effect. The baryon fractions of these galaxies really are different from those derived for clusters of galaxies.

It is not obvious why the baryon fraction should differ from halo to halo. If for the moment we assume our limit to be representative of the universal fraction, then the limits on Ω_b and f_b give $\Omega_0 > 0.45$. However, the methods used

---

[‡] Here we specifically do not include HI and other potentially star forming material; the low $(M/L)_\star$ simply reflects that the LSB has not had enough time to build a large old stellar population as in HSB galaxies.
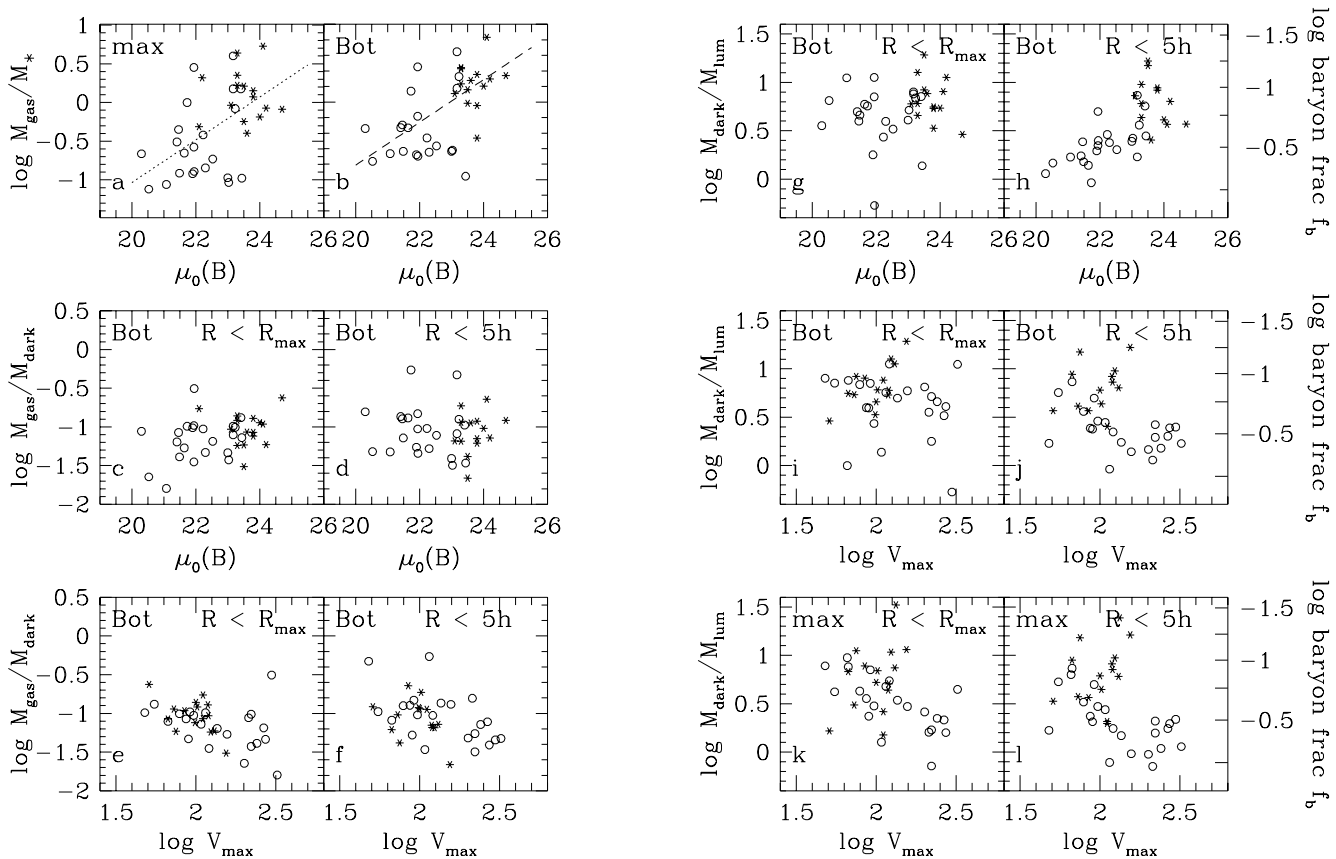
Figure 11. Ratios of the various mass components. All stellar and dark masses are computed as indicated in the panels, where 'max' denotes maximum disk and 'Bot' Bottema disk. The outermost radius R_{max} is defined as the the radius of the last measured point of the rotation curve. h is the disk scale length. Shown are: the ratio of stellar masses and gas masses for maximum disk (**a**), where the dotted line is a least-squares fit to the data; the ratio of stellar masses and gas masses for Bottema disk (**b**); the ratio of gas mass and dark mass as a function of surface brightness μ_0, measured within R_{max} (**c**) and within $5h$ (**d**); the ratio of gas mass and dark mass as a function of maximum rotation velocity V_{max}, measured within R_{max} (**e**) and within $5h$ (**f**); the ratio of dark mass and luminous mass (and baryon fraction) as a function of μ_0, measured within R_{max} (**g**) and within $5h$ (**h**); the ratio of dark mass and luminous mass for the Bottema disk as a function of V_{max}, measured within R_{max} (**i**) and within $5h$ (**j**); the ratio of dark mass and luminous mass for the maximum disk as a function of V_{max}, measured within R_{max} (**k**) and within $5h$ (**l**)

to obtain the cluster results have now been thoroughly analyzed by many groups (e.g. White & Fabian 1995; Evrard et al. 1996) and seem robust.

It may be that f_b really varies from halo to halo, perhaps depending on scale. What physics might cause this is unclear. Dissipation acts in the wrong direction: if galaxies have dissipated a lot, their halos are very large, worsening the problem. It has been suggested that low mass galaxies experience significant wind driven mass loss (e.g. Dekel & Silk 1986) which might rid them of some baryons. However, this clearly has not occurred in the galaxies we are discussing. Their gas has not been swept out; they are very gas rich and massive. They show no evidence of blow-out events (Bothun et al. 1994). It is therefore entirely ad-hoc to vary f_b, and this would add yet another free parameter to the current cosmological models.

Of course, until the nature of the dark matter is known, it is conceivable that some or all of it is baryonic. Thus, another possibility is that some fraction of halos is baryonic, and relatively more baryons have been incorporated into the

halos of LSB galaxies, perhaps as MACHOs. How and why this should occur is again inobvious. LSB galaxies show little evidence of an early epoch of star formation which ought to provide the remnants that become MACHOs (McGaugh & Bothun 1994; de Blok et al. 1995), and it is not obvious that these should be distributed in a halo. Completely non-baryonic matter is still required unless primordial nucleosynthesis or large scale estimates of Ω_0 are wrong. The limits derived from the LSB galaxies are, however, hard limits, and they should be reconciled with the cluster values. If that does not prove to be possible, this might at last resort even indicate the break down of the dark matter hypothesis (Sanders 1997).
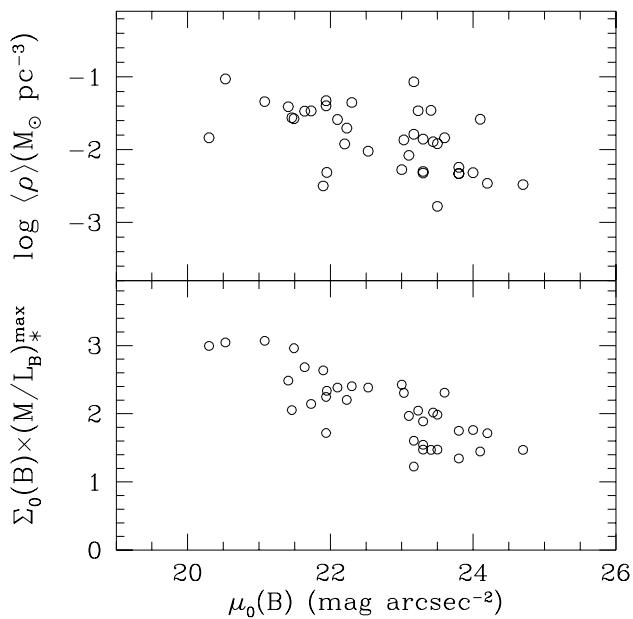
7.2 Maximum disk baryonic surface densities

The maximum disk results are a good way to demonstrate that LSB galaxies have truly low matter surface density disks. That is, they are not normal surface density disks that happen to have less light per square parsec, but the underlying mass surface density distribution is more diffuse too (de Blok & McGaugh 1996).

In Fig 12 we show the central surface densities calculated by multiplying the central surface brightness with the respective $(M/L)_\star$ ratios. The resulting surface density is the maximum density the disk can have within the constraints of the observed rotation curve. These values have not been corrected for the presence of HI, as the surface density of the HI gas becomes progressively lower towards lower surface brightnesses (BMH96). The increase in maximum disk $(M/L)_\star$ ratio is not fast enough to compensate for the decrease in surface brightness: an effect which will only become more pronounced when hypotheses other than maximum disk are used. Maximum disk is the most conservative scenario, but already here it is clear that the mass surface density in the disk is a function of surface brightness.

8 SUMMARY

We have presented rotation curve decompositions of a sample of LSB galaxies and compared the properties of their constituent mass components with those of a sample of HSB galaxies.

LSB galaxies are very much dominated by dark matter thus proving to be the ideal test-cases for theories on the structure and formation of dark matter halos. The halo parameters derived for these galaxies are insensitive to the assumed mass-to-light ratio of the stellar disk, ensuring that the value we derive are in all probability close to the true values.

This is in sharp contrast with HSB galaxies, where the halo parameters are sensitive to the assumed stellar mass-to-light ratio. Comparison of the HSB and LSB samples shows that the maximum disk solutions imply an increasing stellar mass-to-light ratio for the stellar disk and an increasing compactness for the halo as the central surface brightness decreases, while the Bottema disk solutions imply exactly the opposite. We argue, based on what is known about the evolutionary state of LSB galaxies from other sources, that the maximum disk solution is not representative. To explain the maximum disk results in a physical way, one has to assume large amounts of baryonic (dark) matter in the LSB disks. This would result in massive, evolved disks, which is not consistent with the observed past and present low star formation rates of LSB galaxies. The Bottema disk solutions give lower $(M/L)_\star$ values, more consistent with what can be derived from other evolutionary probes (metallicity, gas fraction). They imply that LSB galaxies live in extended diffuse halos. The halos of LSB galaxies are thus fundamentally different from those of HSB galaxies of the same mass. This is a challenge for cosmological N-body simulations which will have to address this problem, especially considering the numerical richness of LSB galaxies.

LSB galaxies are thus slowly evolving, isolated, diffuse, low-density and extremely dark matter dominated galaxies.

Figure 12. Top panel: Average volume density of LSB galaxies as measured within 5 disk scale lengths. Bottom panel: Central mass surface density implied by the maximum disk fits. Both quantities depend on surface brightness.

7 SURFACE AND VOLUME DENSITIES

7.1 Total mass volume densities

A question which remains to be answered is whether the low surface densities now observed in LSB galaxies also imply that they are truly low *volume* density objects. This question is extensively discussed in de Blok & McGaugh (1996) where the LSB galaxy UGC 128 and HSB galaxy NGC 2403 (which lie at identical positions on the TF relation) are compared. The conclusion reached there is that the total mass volume density enclosed within a fixed number of scale lengths is a factor ~ 10 lower in UGC 128 than in NGC 2403. We refer to that work for a discussion on the preferred length scale for measuring densities in galaxies.

We have extended this analysis to our samples of HSB and LSB galaxies. The total mass density within $5h$ was computed and shown as a function of surface brightness in Fig 12. The conclusion reached in de Blok & McGaugh is confirmed: the difference in $\langle\rho\rangle$ between Freeman like galaxies and LSB galaxies with $\mu \simeq 24$ is again a factor of 10.

Although a large range in mass density is inferred at each value of μ_0, LSB galaxies are "diffuse" objects, even in the maximum disk case. The increase in optical scale length towards lower surface brightnesses is much faster than any change in the DM length scale. The increase in area spanned by the optical disk can therefore not be compensated by a corresponding increase in total matter enclosed by the optical disk. The enclosed mass increases with V^2h, while the enclosed area (volume) increases with h^2 (h^3). The increasing scale length therefore ensures that for LSB galaxies the average volume or surface density enclosed by the disk is always lower.

REFERENCES

Ashman, K.M., Salucci, P., Persic, M. 1993, MNRAS, 260, 610

Athannasoula, E., Bosma, A., Papaioannou, S., A&A, 179, 23

Begeman, K.G. 1987, PhD thesis, University of Groningen

Begeman, K.G., Broeils, A.H., & Sanders, R.H. 1991, MNRAS, 249, 523

Bosma, A. 1978, PhD thesis, University of Groningen

Bosma, A., Athanassoula, E. & van der Hulst, J.M. 1988, A&A, 198, 100

Bothun, G.D., Schombert, J.M., Impey, C.D., Sprayberry, D., McGaugh, S.S., 1993, AJ, 106, 530

Bothun, G. D., Eriksen, J., & Schombert, J. M. 1994, AJ, 108, 913

Bothun, G.D., Impey, C., McGaugh, S.S., 1997, PASP, in press

Bottema, R. 1995, PhD thesis, University of Groningen

Bottema, R, 1997, submitted

Broeils, A.H, 1992, PhD thesis, University of Groningen

Corradi, R.L.M., Capaccioli, M. 1990, A&A, 237, 36

Casertano, S. 1983, MNRAS, 203, 735

Casertano, S., van Gorkom, J.H. 1991, AJ, 101, 1231

Dalcanton J.J., Shectman, S.A., 1996, ApJL, 465, L9

Dalcanton J.J., Spergel D.N., Summers F.J., 1997, preprint

David, L.P., Jones, C. & Forman, W. 1995, ApJ, 445, 578

Davies, J.I. 1990, MNRAS, 244,

de Blok, W.J.G., & McGaugh, S.S 1996, ApJL, 469, L89

de Blok W.J.G., van der Hulst J.M., Bothun G.D., 1995, MNRAS, 274, 235

de Blok, W.J.G., McGaugh, S.S, & van der Hulst, J.M. 1996, MNRAS, 283, 18

de Jong, R.S., 1995, PhD thesis, University of Groningen

Dekel, A., & Silk, J. 1986, ApJ, 303, 39

de Vaucouleurs A., de Vaucouleurs G., Buta R.J., Corwin Jr. H.G., Fouqué P., Paturel G., 1991, Third Reference Catalogue of Bright Galaxies (RC3), Springer-Verlag, New York

Evrard, G.A., Metzler, C., & Navarro, J. 1996, ApJ, 469, 494

Fall, S.M., Efstathiou, G., 1990, MNRAS, 192, 189

Freeman K.C., 1970, ApJ, 160, 811

Impey, C., Bothun, G.D., 1997, ARA&A, in press

Jablonka, J., & Arimoto, N., 1992, A&A, 255, 63

Jobin, M., Carignan, C., 1990, AJ, 648

Kalnajs, A.J. 1983, in: *Internal Kinematics of Galaxies, IAU Symposium No. 100*, ed. E. Athanassoula (Dordrecht: Reidel), p. 87

Kennicutt, R.C., Jr. 1989, ApJ, 344, 685

Kent S.M., 1986, AJ, 91, 1301

Kuijken, K., & Gilmore, G., 1989, MNRAS, 239, 571

Lake, G., Feinswog, L. 1989, AJ, 98, 166

Larson, R.B. & Tinsley, B.M., 1978, ApJ, 219, 46

Martimbeau, N., Carignan, C., Roy, J.-R., 1994, AJ, 107, 543

McGaugh S.S. 1992, PhD thesis, University of Michigan

McGaugh S.S., 1994, ApJ, 426, 135

McGaugh, S.S., 1996, MNRAS, 280, 337

McGaugh, S.S., Bothun G.D., 1994, AJ, 107, 530

McGaugh, S.S., & de Blok, W.J.G., 1997, ApJ, in press

McGaugh S.S., Bothun G.D., Schombert J.M., 1995, AJ, 110 573

Milgrom, M. 1983, ApJ, 270,365

Mo, H. J., McGaugh, S.S., Bothun, G. D., 1994, MNRAS, 267, 129

Moore, B. 1994, Nature, 370, 629

Navarro, J.F. 1996, preprint, astro-ph/9610188

Peletier, R.F., Valentijn, E.A., Moorwood, A.F.M., Freudling, W., Knapen, J.H., Beckman, J.E. 1995, A&A, 300, L1

Persic M., Salucci P., 1991, ApJ, 368, 60

Pfenniger D., Combes F., Martinet L., 1994, A&A, 285, 79

Pildis, R.A., Bregman, J.N., & Evrard, A.E. 1995, ApJ, 443, 514

Rönnback, J. & Bergvall, N. 1994, A&AS, 108, 193

Rönnback, J. & Bergvall, N. 1995, A&A, 302, 353

Sanders, R.H. 1997, ApJ, in press

Schombert J.M., Bothun G.D., Impey C.D., Mundy L.G., 1990, AJ, 100,1523

Schombert, J.M., Bothun, G.D., Schneider, S.E., McGaugh, S.S., 1992, AJ, 103, 1107

Rhee, M-H, 1996, PhD thesis, University of Groningen

Rubin, V.C., Boss, A.P., Ford, W.K, Jr. & Kenney, J.D. 1989,AJ,98,1246

van Albada, T.S, Sancisi, R., 1986, Phil. Trans. R. Soc. Lond. A, 320, 447

van Albada, T. S., Bahcall, J. N., Begeman, K. & Sanscisi, R. 1985, ApJ, 295, 305

van den Hoek, L.B., de Blok, W.J.G., van der Hulst, J.M., de Jong, T., A&A, submitted

van der Hulst J.M., Skillman E.D., Smith T.R., Bothun G.D., McGaugh S.S., de Blok W.J.G., 1993, AJ, 106, 548

van der Kruit, P.C., & Searle, L. 1981, A&A, 95, 105

van der Kruit, P.C., 1986, A&A, 157, 230

Walker, T.P., Steigman, G., Schramm, D.N., Olive, K.A., & Kang, H. 1991, ApJ, 376, 51

White, D.A., & Fabian, A.C. 1995, MNRAS, 273, 72

White, S.D.M., Navarro, J.F., Evrard, A.E., & Frenk, C.S. 1993, Nature, 366, 429

Zwaan M.A., van der Hulst J.M., de Blok W.J.G., McGaugh S.S., 1995, MNRAS, 273, L35

APPENDIX A1: THE GENERALIZED BOTTEMA-DISK

A1.1   Introduction

Bottema (1995) has shown from measurements of the stellar velocity dispersions in a sample of HSB galaxies that the maximum rotation velocity of the stellar disk (i.e. the velocity occuring at $2.2h$) is on average equal to 63% of the measured rotation velocity at that radius.

This result was derived under the explicit assumption of Freeman's Law (which applies to most of the galaxies in Bottema's sample). It is therefore not possible to directly apply Bottema's result to our sample of LSB galaxies, especially if one realizes that 63% of the observed rotation velocity in many LSB galaxies exceeds the maximum disk solution.

In Bottema (1997) a re-analysis and generalization of these results is presented, also taking into account surface brightness and color effects. We here summarize the main points of that analysis.

A1.1.1 Poor man's population synthesis

The disk is assumed to be unaffected by dust and contains only two populations (van der Kruit 1986; Bottema 1988): a young component with a color $(B-V)^y = -0.03$ and an old component with $(B-V)^o = 0.97$. The old component furthermore contains all of the disk mass.

It is straightforward to show that this implies that $S_V^y = 0.973 S_B^y$ and $S_V^o = 2.44 S_B^o$, where $S_{B,V}$ are the fluxes of the old and young populations in the B and V bands.

The absolute magnitude of the old disk in the B-band, M_B^{od}, is related to the total absolute magnitude M_B^{tot} by

$$M_B^{od} = M_B^{tot} - 2.5 \log(S_B^y/S_B^{tot}) \tag{A1}$$

It is straightforward to show that this equation and the colors of the populations imply that

$$M_{od}^B = M_B - 2.5 \log\left(\frac{1 - 0.973 \cdot A^\star}{1.467 \cdot A^\star}\right) = M_B - cf, \tag{A2}$$

where $A^\star$ is defined as $10^{-0.4(B-V)}$.

A1.1.2 The exponential disk

For an exponential, locally isothermal, constant M/L disk with density distribution $\rho(R,z) = \rho(R,0)\operatorname{sech}^2(z/z_0)$, and

$$\langle v_z^2 \rangle_{R=0}^{\frac{1}{2}} = \sqrt{\pi G \sigma_0 z_0}, \tag{A3}$$

and

$$\langle v_z^2 \rangle_{R=0}^{\frac{1}{2}} = \sqrt{\pi G \, \Sigma_0 \left(\frac{M}{L}\right) z_0}, \tag{A4}$$

where $\langle v_z^2 \rangle_{R=0}^{\frac{1}{2}}$ is the central velocity dispersion, and σ_0, Σ_0 and z_0 are the central surface density, surface brightness and scale height, respectively.

For an infinitely thin stellar disk the maximum rotation velocity is given by

$$v_{\max} = 0.88\sqrt{\pi G \, \sigma_0 h}. \tag{A5}$$

Combining Eqs. (A4) and (A5) yields

$$v_{\max} = 0.88 \, \langle v_z^2 \rangle_{R=0}^{\frac{1}{2}} \sqrt{\frac{h}{z_0}}. \tag{A6}$$

A1.1.3 The old-disk Tully-Fisher relation

Equation (A5) and the identity $L = 2\pi\Sigma_0 h^2$, where L is the total luminosity, Σ_0 the central surface brightness in linear units, and h the scale length, imply an old disk Tully-Fisher relation

$$v_{\max,od}^4 = 0.3\pi G^2 \Sigma_0^{od}\left(\frac{M}{L}\right)_{od}^2 L_{od} \tag{A7}$$

As the old disk contains all the mass $v_{\max,od}^4 = v_{\max}^4$. $(M/L)_{od}$ is assumed to be the the same for all old disks.

A1.2 Bottema disk for Freeman galaxies

For Freeman galaxies μ_0 is constant. The color is also assumed to be constant at $B - V = 0.7$. Eq. (A7) then yields $M_{od} = -10\log(v_{\max}) + C$, or

$$v_{\max} = 10^{0.1C} 10^{-0.1 M_{od}}. \tag{A8}$$

Combining Eqs. (A6) and (A8) yields

$$\langle v_z^2 \rangle_{R=0}^{\frac{1}{2}} = A^{-1}\sqrt{\frac{z_0}{h}}\, 10^{-0.1 M_{od}}, \tag{A9}$$

where A is defined as

$$A = 0.88 \cdot 10^{-0.1C}. \tag{A10}$$

Following Bottema (1995) the empirical relation between luminosity and scale length ratios is adopted $h/z_0 = 0.6\,M_{od} + 17.5$ together with the corresponding values $A = 0.75$, $C = 0.69$ and $(M/L_B) = 1.85$. This results in

$$v_{\max} = 1.17 \cdot 10^{-0.1 M_{od}}. \tag{A11}$$

A1.3 General Bottema disk for non-Freeman galaxies

The result derived above strictly speaking only applies to galaxies that obey Freeman's Law. To generalize to different surface brightnesses rewrite Equation (A7) as

$$v_{\max}^4 = 0.3\pi G^2 \Sigma_{0,F}\left(\frac{\Sigma_0^{od}}{\Sigma_{0,F}}\right)\left(\frac{M}{L}\right)_{od}^2 L_{od}, \tag{A12}$$

where $\Sigma_{0,F}$ is the constant Freeman central surface brightness of $136\,L_\odot\,\mathrm{pc}^{-2}$. The scale lengths of the old and young populations are assumed to be equal, so that $\Sigma_0^{od}/\Sigma_0 = L_{od}/L_{tot} = 10^{0.4cf}$. This results in

$$v_{max} = \mathrm{const}\left(\frac{\Sigma_0}{\Sigma_{0,F}}\right)^{\frac{1}{4}} 10^{0.1cf} 10^{-0.1 M_{od}} \tag{A13}$$

For Bottema's sample, with central surface brightnesses approximately equal to the Freeman value and colors close to $B - V = 0.7$, an average correction factor $\langle cf \rangle \simeq -0.5$ can be defined. Combination of Eqs (A6) and (A13) then yields

$$\langle v_z^2 \rangle_{R=0}^{\frac{1}{2}} = \frac{\mathrm{const}}{0.88}\sqrt{\frac{z_0}{h}}\left(\frac{\Sigma_0}{\Sigma_{0,F}}\right)^{\frac{1}{4}} \frac{10^{0.1(cf + \langle cf \rangle - M_{od})}}{10^{0.1\langle cf \rangle}} \tag{A14}$$

Again using Bottema's relation $h/z_0 = 0.6 M_{od} + 17.5$ then implies that

$$\mathrm{const} \times 10^{0.1\langle cf \rangle} = 1.17$$

For the maximum rotation velocity and velocity dispersion of a galactic disk one then finds (using Eqs. (A13) and (A14))

$$v_{\max} = 1.17\left(\frac{\Sigma_0}{\Sigma_{0,F}}\right)^{\frac{1}{4}} \cdot 10^{0.1(cf - \langle cf \rangle)} 10^{-0.1 M_{od}}, \tag{A15}$$

and

$$\langle v_z^2 \rangle_{R=0}^{\frac{1}{2}} = 1.33\sqrt{\frac{z_0}{h}}\left(\frac{\Sigma_0}{\Sigma_{0,F}}\right)^{\frac{1}{4}} 10^{0.1(cf - \langle cf \rangle - M_{od})} \tag{A16}$$

Conversion to observables using Eq (A2) then yields

$$v_{\max} = 1.17\left(\frac{\Sigma_0}{\Sigma_{0,F}}\right)^{\frac{1}{4}} \cdot 10^{0.2(cf + 0.25)} 10^{-0.1 M_B^{tot}}, \tag{A17}$$

A1.4   Mass-to-light ratio

From Eqs. (A4) and (A16) one can derive that

$$\left(\frac{M}{L}\right)_B = 28.1 \cdot 10^{-0.2 M_{B,\odot}} \cdot 10^{0.4 cf} 10^{-0.2 \langle cf \rangle}, \qquad \text{(A18)}$$

With $M_{B,\odot} = 5.48$ one finds

$$\left(\frac{M}{L}\right)_B = 1.79 \cdot 10^{0.4 cf} 10^{0.2(0.5 - \langle cf \rangle)} = 2.84 \cdot 10^{0.4 cf}$$

$$= 1.936 \cdot 10^{0.4(B-V)} - 1.883. \qquad \text{(A19)}$$

The mass-to-light ratio does not depend on the surface brightness of the disk, which is due to our assumption that the old disk population has the same mass-to-light ratio for all disks. Disks with identical colors therefore have identical mass-to-light ratios, irrespective of surface brightness.